

1 **CHIP ubiquitin ligase is involved in the nucleolar stress management**

2
3 Authors: Malgorzata Piechota^{1*}, Lilla Biriczova^{1†}, Konrad Kowalski^{1†}, Natalia A. Szulc¹,
4 Wojciech Pokrzywa^{1*}

5
6 ¹Laboratory of Protein Metabolism, International Institute of Molecular and Cell Biology
7 in Warsaw, Poland

8
9 * Correspondence should be directed to:

10 WP: wpokrzywa@iimcb.gov.pl

11 MP: mpiechota@iimcb.gov.pl

12
13 † These authors contributed equally to this work

14 15 **ABSTRACT**

16 The nucleolus is a dynamic nuclear biomolecular condensate involved in cellular stress
17 response. Under proteotoxic stress, the nucleolus can store damaged proteins for
18 refolding or degradation. HSP70 chaperone is a well-documented player in the
19 recovery process of proteins accumulated in the nucleolus after heat shock. However,
20 little is known about the involvement of the ubiquitin-proteasome system in the turnover
21 of its nucleolar clients. Here we show that HSP70, independently of its ATPase activity,
22 promotes migration of the CHIP (carboxyl terminus of HSC70-interacting protein)
23 ubiquitin ligase into the granular component of the nucleolus, specifically after heat
24 stress. We show that while in the nucleolus, CHIP retains mobility that depends on its
25 ubiquitination activity. Furthermore, after prolonged exposure to heat stress, CHIP self-
26 organizes into large, intra-nucleolar droplet-like structures whose size is determined
27 by CHIP ubiquitination capacity. Using a heat-sensitive nucleolar protein luciferase, we
28 show that excess CHIP impairs its regeneration, probably through deregulation of
29 HSP70. Our results demonstrate a novel role for CHIP in managing nucleolar
30 proteostasis in response to stress.

31 32 **KEYWORDS**

33
34 nucleolus; heat stress; proteostasis; CHIP; HSP70

35 36 **INTRODUCTION**

37
38 The nucleolus is the largest subnuclear compartment formed by immiscible liquid
39 phases that control ribosome biogenesis and translational capacity (Feric et al., 2016).
40 It consists of three distinct layers: the fibrillar center (FC), dense fibrillar component
41 (DFC) and granular component (GC), which surrounds FC and DFC, and the
42 perinucleolar compartment (PNC) (Biggiogera et al., 1990; Feric et al., 2016). FC-DFC
43 interface is a site where ribosomal DNA (rDNA) is actively transcribed, while DFC
44 contains proteins such as fibrillarin, which are essential for rDNA processing (Jordan,
45 1984; Scheer and Hock, 1999; Smirnov et al., 2014; Lafontaine et al., 2021). GC is
46 abundant in nucleophosmin (NPM1) and nucleolin proteins (Biggiogera et al., 1990)
47 and acts as a site of ribosome subunits assembly (Feric et al., 2016; Kozakai et al.,
48 2016; Mitrea et al., 2018). In addition, the nucleolus can serve as a safe harbor for

49 proteins after exposure to environmental stimuli or stress factors. For example, labile
50 proteins during heat stress are transported into the nucleolus, where the heat shock
51 protein 70 (HSP70) protects them from aggregation and facilitates their extraction and
52 refolding after stress (Nollen et al., 2001; Frottin et al., 2019). Thus, the HSP70
53 chaperone is essential for the maintenance of nucleolar proteostasis. Recent
54 proteomic analysis of the nucleolus from heat-shock treated cells identified numerous
55 proteins accumulating in nucleoli among which several belonged to the ubiquitin-
56 proteasome system (UPS) (Azkanaz et al., 2019). UPS regulates various cellular
57 pathways by removing unwanted and damaged proteins marked by a small protein –
58 ubiquitin (Ub). Its attachment is mediated by the Ub-activating enzymes (E1), Ub-
59 conjugating enzymes (E2), and Ub ligases (E3) that select target proteins. In most
60 cases, the proteasome subsequently degrades ubiquitinated proteins (Komander,
61 2009; Buetow and Huang, 2016). However, little is known about the involvement of the
62 UPS in nucleolar stress response and proteostasis maintenance. Recent studies
63 identified numerous proteins bound to NPM1 after heat shock (Frottin et al., 2019).
64 Their accumulation was transient, only under heat shock, and HSP70 activity was
65 required for their dissociation from NPM1 during recovery (Frottin et al., 2019).
66 Interestingly, several E3 ligases were detected in the aforementioned study, but further
67 investigation of their nucleolar functions was not carried out. One of these was the
68 quality control E3 ligase CHIP (C-terminus of Hsc70-interacting protein), the well-
69 known HSP70 interactor. CHIP contains three tandem tetratricopeptide repeat (TPR)
70 motifs that bind to the HSP70 and HSP90 chaperones and the catalytic U-box domain
71 responsible for substrate ubiquitination (Ballinger et al., 1999; Jiang et al., 2001). Early
72 work showed that heat-treated CHIP retains its ubiquitination activity and can modify
73 substrates bound to HSP70/HSC70 (Ballinger et al., 1999; Meacham et al., 2001;
74 Murata et al., 2001; Shimura et al., 2004; Tateishi et al., 2004; Younger et al., 2004;
75 Stankiewicz et al., 2010). In addition, CHIP can control HSP70 levels in the client-free
76 state through ubiquitination or by activating the transcription factor HSF1, a key
77 regulator of the heat shock response (HSR) in eukaryotic cells (Dai et al., 2003; Qian
78 et al., 2006). In mouse fibroblasts where CHIP was knocked out, heat-induced HSP70
79 activation was significantly reduced. On the other hand, its turnover rate also
80 decreased, indicating that HSP70 and CHIP closely collaborate on degrading the
81 chaperone's substrates, and their interaction is also self-regulatory (Dai et al., 2003;
82 Qian et al., 2006). However, it is unclear what is the role of CHIP while in the nucleolus
83 and whether it also cooperates with HSP70 in maintaining nucleolar proteostasis
84 during heat stress and recovery.

85
86 Here we show that heat shock-induced CHIP migration to nucleoli depends on HSP70
87 presence but not its activity. Nevertheless, functional HSP70 is essential for the
88 release of CHIP from the nucleolus. We also noted that nucleolar CHIP could exhibit
89 ubiquitination activity during heat stress and recovery. Specifically, CHIP is recruited
90 to the GC compartment where it acts as a non-aggregating protein; however, its
91 mobility becomes significantly limited when deprived of ubiquitination ability.
92 Remarkably, CHIP localizes to specific condensates generated in the nucleolus under
93 prolonged heat stress and whose dynamics depend on its E3 activity. To this end, we
94 used luciferase as a stress-sensitive model protein sorted to the nucleolus during heat
95 shock and observed that CHIP hinders its regeneration, likely in collaboration with
96 HSP70. Our results provide the groundwork for further studies on CHIP function in a
97 nucleolar heat stress response.

98

99 RESULTS

100 101 **CHIP translocates to nucleoli in heat-stressed cells**

102
103 To investigate the localization and function of CHIP in heat-stressed cells, we
104 established two cell lines, based on the Flp-In system compatible HeLa and HEK-293
105 cells (Szczeny et al., 2018), stably overexpressing CHIP tagged with the EGFP
106 fluorescent marker (hereafter HeLa EGFP-CHIP and HEK EGFP-CHIP cells) (Fig.
107 S1A). In the experiment we exposed cells to heat shock at 42°C for 90 min, followed
108 by recovery period at 37°C for 2 h (Fig. 1A). We found that EGFP-CHIP localized to
109 nucleoli in both cell lines, specifically during heat shock, and abandoned it upon
110 recovery (Fig.1B, Fig. S1B). None of the other tested stressors, such as arsenite,
111 sorbitol, thapsigargin, or puromycin, induced CHIP migration into the nucleolus (Fig.
112 S1B). We further confirmed the ability of CHIP to translocate into nucleoli in MCF7
113 breast cancer cells transiently transfected with EGFP-CHIP (Fig. S1C). Importantly,
114 endogenous CHIP also accumulated in the nucleolus after heat shock in HeLa Flp-In
115 and MCF7 cells (Fig. 1C and S1D), indicating that CHIP translocation to the nucleolus
116 is not an artifact resulting from EGFP tagged protein overexpression. Quantification of
117 endogeneous CHIP intensities across nuclei and nucleoli in MCF7 cells confirmed its
118 increased nucleolar localization during heat stress (Fig. S1E).

119
120 Next, we fractionated HeLa Flp-In cells into cytoplasmic, nucleoplasmic, and nucleolar
121 fractions to verify CHIP translocation into nucleoli. Consistent with our imaging data,
122 we found elevated CHIP levels in the nucleolar fractions of heat-stressed cells (Fig.
123 1D). Importantly, we also detected elevated levels of HSP70 chaperone in nucleolar
124 fractions after heat shock, which is consistent with previous reports (Pelham et al.,
125 1984; Pelham, 1984; Welch and Feramisco, 1984; Welch and Suhan, 1986; Nollen et
126 al., 2001; Azkanaz et al., 2019; Frottin et al., 2019). Following the suggestion that
127 HSP70 may enter nucleoli in complex with other proteins (Frottin et al., 2019), we
128 determined whether it modulates CHIP translocation into nucleoli. To verify this, we
129 examined the transport of the CHIP K30A mutant, which is deficient in HSP70 binding.
130 Indeed, HeLa Flp-In cells transiently transfected with the EGFP-CHIP K30A mutant
131 exhibited impaired CHIP migration to nucleoli after heat shock (Fig. 1E). Therefore, we
132 further aimed to determine the role of HSP70 in CHIP nucleolar localization.

133 134 **HSP70-dependent localization of CHIP in nucleoli**

135
136 HSP70 colocalizes with CHIP in the nucleoli of heat-treated HeLa EGFP-CHIP cells,
137 suggesting their functional cooperation (Fig. 2A). To examine the role of HSP70 in
138 nucleolar CHIP accumulation, we lowered the HSP70 level via siRNA silencing in HeLa
139 EGFP-CHIP cells (Fig. S2A) and applied our heat shock scheme (Fig. 1A). We
140 observed reduced CHIP migration to the nucleoli in these cells (Fig. 2B). Furthermore,
141 depleting HSP70 hindered CHIP exit from nucleoli during regeneration where 2 h post-
142 heat shock more than 60% of cells still maintained CHIP in nucleoli, compared to
143 approximately 10% of control cells (Fig. 2B and 2C).

144
145 We next monitored CHIP localization during heat shock and recovery in the presence
146 of VER-155008 (hereafter VER), a small molecule inhibitor of HSP70, to test whether
147 HSP70 activity is required for CHIP translocation to nucleoli. Notably, we used 40 μ M
148 VER in HeLa EGFP-CHIP and MCF7 cells as this concentration was successfully

149 applied to inhibit HSP70 activity in HeLa cells during recovery from the 3 h heat shock
150 (Mediani et al., 2019). We observed CHIP levels gradually increasing in the nucleoli of
151 HeLa EGFP-CHIP and MCF7 cells during heat shock, implying that its nucleolar
152 migration was not affected by HSP70 inhibition (Fig. 2D and S1E). However,
153 continuous VER treatment during heat shock and recovery blocked CHIP release
154 during recovery, which resembled the effect of HSP70 depletion (Fig. 2D and S1E).
155 These results suggest that HSP70 recruits CHIP in an activity-independent manner
156 upon entry to the nucleolus, but its functional operability in this compartment is required
157 for the recovery process and consequent CHIP release. When VER was provided only
158 during the recovery stage, CHIP clearance from nucleoli was only slightly reduced (Fig.
159 2E), indicating that CHIP trapping in nucleoli depends primarily on the functionality of
160 the HSP70 during heat shock.

161
162 Therefore, we wanted to determine whether CHIP in the nucleolus acts as a functional
163 protein or as the HSP70 substrate, misfolded upon heat shock. Based on observations
164 that misfolded proteins acquire low mobility in the nucleolus (Azkanaz et al., 2019;
165 Frottin et al., 2019), we analyzed CHIP nucleolar fraction mobility in untreated cells
166 and in the presence of VER by recording fluorescence recovery after photobleaching
167 (FRAP). Approximately 70% of EGFP-CHIP sequestered in nucleoli after heat shock
168 was mobile, and HSP70 inhibition did not significantly reduce its dynamics (Fig. 2F).
169 CHIP mobility was also unchanged after 1 h post-heat shock recovery in the presence
170 of VER (Fig. 2G). This indicates that CHIP can form a functional, unaggregated protein
171 in the nucleoli.

172 173 **Nucleolar CHIP colocalizes with the NPM1-containing granular component (GC)** 174 **phase**

175
176 The organization of the nucleolus, involving all three layers, is essential for its role in
177 ribosome biogenesis (Huang, 2002; Krüger et al., 2007; Riback et al., 2020). In turn,
178 the GC is thought to be the main phase supporting misfolded proteins translocated
179 there during proteotoxic stress (Azkanaz et al., 2019; Frottin et al., 2019). To study
180 CHIP specific localization in the nucleolus, we performed colocalization analysis using
181 confocal microscopy with the Airyscan detector, contributing to the improved image
182 resolution (Wu and Hammer, 2021). HeLa EGFP-CHIP cells were stained for NPM1,
183 a GC marker, and fibrillarin (FBL), a DFC marker. Under heat shock and recovery
184 conditions, with or without VER, CHIP colocalized with NPM1 (Fig. 3A and 3C) and, to
185 a much lesser extent, with FBL (Fig. 3B and 3C), suggesting potential CHIP
186 involvement in protein quality control processes in GC.

187 188 **CHIP import to nucleoli is not induced by nucleolar stress *per se***

189
190 To investigate whether CHIP migration to the nucleolus can be triggered as a result of
191 nucleolus impairment, we treated cells with low doses of the transcription inhibitor
192 Actinomycin D (hereafter Act D), which alters the distribution of multiple nucleolar
193 proteins, resulting in the formation of nucleolar caps (Reynolds et al., 1964; Shav-Tal
194 et al., 2005). Act D altered the morphology of nucleoli, causing their circularization,
195 reduction in size, and the formation of FBL nucleolar caps (Fig. S3A and S3B).
196 However, it did not induce CHIP migration to nucleoli (Fig. 4A-C). These results support
197 the concept that CHIP is involved in the nucleolar heat stress response process rather
198 than, for example, suppressing rRNA transcription defects. While treatment with Act D

199 prior to heat shock did not affect CHIP migration to nucleoli (Fig. 4B and 4C), it altered
200 CHIP distribution, which more prominently overlapped with Act D-induced NPM1 ring
201 formations (Fig. 4D). In addition, in cells exposed to Act D, CHIP exit from the nucleolus
202 during the 2 h heat stress recovery was partially impaired (Fig. 4B, 4C and S3C). This
203 observation suggests that proper nucleolar assembly may be necessary for CHIP
204 dynamics.

205

206 **CHIP activity promotes its dynamics in the nucleolus**

207

208 We used a modified *in vitro* ubiquitination assay using total cell lysate as a CHIP source
209 to verify if CHIP activity is maintained in nucleoli. This assay is based on the ability of
210 an E3 ligase to self-ubiquitinate in the presence of the complete ubiquitination
211 enzymatic cascade, namely E1 ubiquitin-activating enzyme, E2 ubiquitin-conjugating
212 enzyme, and E3 ligase of interest, with the addition of ubiquitin and ATP, and was
213 repeatedly used to assess CHIP activity in other studies (Murata et al., 2001; Das et
214 al., 2021). We found that neither heat shock nor recovery period affected CHIP
215 ubiquitination activity (Fig. 5A). This is in line with the mobile and unaggregated
216 nucleolar fraction of CHIP (Fig. 2F and G) and implies its capability of performing self-
217 or substrates' ubiquitination. We also investigated whether CHIP activity is required for
218 its translocation using the catalytically-inactive CHIP H260Q mutant (Hatakeyama et
219 al., 2001). We found that the activity of CHIP is not indispensable for heat shock-
220 induced migration to the nucleolus (Fig. 5B). However, FRAP analysis of the nucleolar
221 CHIP H260Q mutant showed a decrease in its dynamics compared to CHIP WT,
222 suggesting that its propensity to aggregate is likely mediated by the loss of
223 ubiquitination activity (Fig. 5C and 5D).

224

225 Nucleoli are sites for immobilization of proteins under heat stress, leading to
226 occurrence of nucleolar foci with an amyloid-like character (Wang et al., 2019). To gain
227 better insight into the long-term impact of proteotoxic stress on CHIP association with
228 nucleoli and the consequences of its inactivity on this process, we subjected cells to
229 prolonged heat shock. Interestingly, sizeable intra-nucleolar CHIP droplet-like
230 structures could be observed after overnight heat shock in cells expressing the CHIP
231 H260Q mutant, outnumbering their WT protein counterparts (Fig. 5E-I). These
232 differences between CHIP WT and mutant assemblies may stem from the alterations
233 in CHIP H260Q dynamics within the nucleolus (Fig. 5C and D). However, we do not
234 know specific biophysical state and function of these structures.

235

236 **CHIP overexpression affects the nucleolar luciferase recovery**

237

238 To investigate whether CHIP abundance in nucleoli can affect the fate of misfolded
239 proteins sorted there, we employed thermolabile luciferase as a model protein since
240 early reports showed that CHIP could control its heat shock-denatured state (Ballinger
241 et al., 1999; Murata et al., 2001; Kampinga et al., 2003; Rosser et al., 2007). To this
242 end, we used the HEK293T cell line permanently expressing a fusion protein of firefly
243 luciferase and heat-stable green fluorescent protein (GFP) carrying an N-terminal
244 nuclear localization signal (hereafter luciferase) (Frottin et al., 2019). This luciferase
245 translocates to nucleoli after heat shock and relocates to the nucleoplasm during
246 recovery. We verified a similar luciferase shuttle using our heat shock/recovery
247 scheme (Fig. 1A) and noted that transiently overexpressed CHIP (tagged with
248 mCherry) colocalizes with luciferase during heat shock (Fig. 6A). To investigate the

249 role of CHIP in nucleolar luciferase processing, we expressed its K30A and H260Q
250 mutants, which inhibit HSP70 binding or CHIP activity, respectively, in the
251 aforementioned HEK293T cell line. As a proxy for luciferase abundance and
252 regeneration, we analyzed the number of its foci in nucleoli during heat shock and the
253 6 h recovery period (Fig. S4A). Luciferase foci number decreased progressively during
254 the recovery, but in cells expressing specifically CHIP WT or CHIP H260Q, their
255 regeneration was slower than in untransfected and mCherry controls (Fig. S4A).
256 Notably, in cells expressing the CHIP H260Q mutant luciferase recovery was not
257 completed within the experimental 6 h time frame. This could be due to the high
258 number of cells containing heat shock-induced luciferase foci and their presence in
259 about 20% of non-heat shocked cells, suggesting that loss of CHIP activity had a potent
260 destabilizing impact on luciferase. Therefore, we decided to normalize our data to
261 correct for the differences in the number of luciferase foci during heat shock and control
262 conditions, focusing explicitly on the ability of CHIP variants to affect luciferase
263 nucleolar regeneration. Our analysis revealed that the elevated CHIP level induced a
264 delay in the dissolution of nucleolar luciferase foci during recovery (Fig. 6B).
265 Overexpression of CHIP WT and CHIP H260Q had the most potent effect on reducing
266 luciferase exit from the nucleolus, and there was no difference in the rate of luciferase
267 recovery between the two variants. In contrast, overexpression of the CHIP K30A
268 mutant exerted a marginal effect on this process (Fig. 6B). When we transfected cells
269 with lower amounts of plasmids to induce milder overexpression of CHIP variants and
270 examined the first two hours of recovery from heat shock, we still observed comparable
271 inhibition of decline of luciferase foci during recovery by CHIP WT and the H260Q
272 mutant and no significant effect of CHIP K30A (Fig. S4B). We assumed that this was
273 due to the inefficient transport of CHIP K30A to nucleoli, as in HeLa Flp-In cells (Fig.
274 1E). Surprisingly, we found comparable redistribution of all CHIP variants to nucleoli
275 during heat shock, suggesting an alternative pathway for CHIP recruitment to nucleoli
276 unaccompanied by HSP70 in HEK293T cells (Fig. 6C). Hence, the above results
277 suggest that the slowed resolution of luciferase foci in nucleoli may be related to cross-
278 talk between CHIP and HSP70.

279
280 We next assessed luciferase levels as the ratio of its intensity between nucleolus and
281 nucleoplasm, as measured immediately after heat shock and during the 6 h recovery
282 period. The distribution of luciferase in untransfected or mCherry-transfected control
283 cells was predominant in the nucleoplasm already at the initial stage of recovery.
284 However, in cells overexpressing CHIP WT, the nucleolar luciferase signal was still
285 noticeable after 3 h of recovery, again indicating that the regeneration rate of luciferase
286 was disrupted (Fig. 6D). While the CHIP K30A mutant showed the least disruption in
287 the redistribution of luciferase, the CHIP H260Q mutant resulted in its most extended
288 nucleolar persistence (Fig. 6D). We also observed that CHIP was leaving the nucleoli
289 during recovery, concomitantly with nucleolar luciferase disappearance, with the
290 slowest rate for the CHIP H260Q mutant (Fig. 6C). Thus, we assume that CHIP-
291 dependent ubiquitination may contribute to luciferase processing in nucleoli and
292 regeneration efficiency.

293
294 As prolonged heat shock was shown to compromise nucleolar quality control and
295 inhibit luciferase regeneration (Frottin et al., 2019), we set out to investigate the effects
296 of CHIP on regeneration under these conditions. We measured luciferase intensity in
297 nuclei and nucleoli and monitored the number of luciferase foci during the 6 h heat
298 shock at 42°C. Control cells and cells expressing CHIP K30A, but not cells expressing

299 CHIP WT and H260Q, were capable of almost complete dissolution of luciferase foci
300 (Fig. S5A, S5B). However, we observed sustained sequestration of CHIP H260Q into
301 nucleoli after prolonged heat stress (Fig. S5C). Thus, we concluded that CHIP
302 repressed rather than enhanced nucleolar luciferase regeneration. Furthermore, our
303 results on CHIP K30A suggest that the interaction of CHIP with HSP70 may play a role
304 in modulating the nucleolus regeneration capacity and CHIP translocation to the
305 nucleoplasm.

306

307 **HSP70 inhibition aggravates the negative effect of CHIP on luciferase** 308 **regeneration**

309

310 We next examined the effect of CHIP on luciferase regeneration in the presence of
311 VER, the HSP70 inhibitor. Cells were treated with VER only during post-heat shock
312 recovery, and the number of nucleolar luciferase foci was measured after 1 h and 2 h
313 of recovery. In untransfected cells, we did not record any impact of VER on luciferase
314 regeneration. Cells overexpressing CHIP WT showed mildly impaired nucleolar
315 luciferase regeneration in the presence of VER, which became apparent after the
316 second hour of recovery compared to condition where it was absent (Fig. 7A).
317 However, overexpression of the CHIP K30A in cells with added VER had a more
318 disruptive effect relative to untreated cells (Fig. 7B). The result for the CHIP K30A
319 mutant was unexpected as, unlike the WT protein, it should not interfere with the
320 HSP70 function, which may suggest the emergence of additional effects associated
321 with the chaperone inhibition. Since the negative effect on luciferase regeneration in
322 CHIP H260Q-expressing cells was also potently enhanced by HSP70 inhibition, we
323 speculate that protection against protein aggregation in the nucleolus requires a
324 balance between HSP70 and E3 CHIP activity.

325

326 **DISCUSSION**

327

328 The nucleolus possesses numerous functions, including ribosome biogenesis, nuclear
329 organization, regulation of global gene expression, and energy metabolism (Cerqueira
330 and Lemos, 2019). It also responds to multiple stresses, such as hypoxia, pH
331 fluctuations, redox stress, DNA damage, or proteasome inhibition, and acts as a
332 protein quality control center that can mitigate heat shock-induced proteotoxicity
333 (Mekhail et al., 2005; Latonen et al., 2011; Audas et al., 2012; Yang et al., 2016;
334 Lindström et al., 2018; Alberti and Carra, 2019; Azkanaz et al., 2019; Frottin et al.,
335 2019; Mediani et al., 2019; Szaflarski et al., 2022). In our studies, we focused on the
336 latter function. It was previously suggested that the nucleolus creates a favorable
337 environment for the HSP70-mediated protection and recovery of heat stress-sensitive
338 proteins (Nollen et al., 2001; Azkanaz et al., 2019; Frottin et al., 2019; Mediani et al.,
339 2019). These include the epigenetic modifier family of Polycomb group (PcG) proteins
340 and the exogenous thermolabile luciferase (Azkanaz et al., 2019; Frottin et al., 2019).
341 In addition, Frottin et al. demonstrated reversible accumulation of CDK1 and BRD2
342 proteins in the nucleolus under heat stress, and Mediani et al. pointed to DRiPs
343 (defective ribosomal products) accumulating in the nucleolus that undergoes reversible
344 amyloidogenesis after heat shock or proteasome inhibition (Frottin et al., 2019; Mediani
345 et al., 2019). To better understand the proteotoxic stress-dependent management of
346 proteins in the nucleolus, we set out to study the protein quality control ubiquitin ligase
347 CHIP, which is well known for its role in ubiquitination of HSP70 substrates, and whose
348 presence in the nucleolus after heat stress has been reported in recent proteomic

349 analyses (Demand et al., 2001; Petrucelli et al., 2004; Joshi et al., 2016; Azkanaz et
350 al., 2019; Frottin et al., 2019).

351
352 We found that CHIP translocation to the nucleolus was caused by heat stress but not
353 by Act D, ruling out a direct CHIP response to transcriptional stress and inhibition of
354 rRNA transcription. CHIP migration was partially dependent on HSP70; however, its
355 chaperone activity was not required. Of note, it was previously reported that the HSP70
356 inhibitor, VER, does not inhibit heat shock-induced nucleolar accumulation of the
357 HSP70 substrate, PcG protein (GFP::CBX2) (Azkanaz et al., 2019). VER competes
358 with ATP and ADP for binding to HSP70 and reduces the rate of nucleotide association
359 and ATP-induced substrate release (Schlecht et al., 2013), but there are no studies on
360 the effect of this compound on HSP70-CHIP complex formation and stability. Thus,
361 although our data show that HSP70 inhibition did not affect CHIP migration to the
362 nucleolus, further studies are needed to elucidate this mechanism. It may be
363 questioned whether the accumulation of CHIP in the nucleolus implies that it is the
364 HSP70 substrate that undergoes chaperone protection and is refolded during
365 regeneration before being released from this compartment. Our FRAP analysis
366 showed that approximately 30% of total CHIP was immobile in the nucleolus in the
367 HeLa EGFP-CHIP cells. Heat shock also induces a similar formation of the immobile
368 GFP-NPM1 protein fraction, which implies altered properties of the GC due to its
369 association with misfolded proteins that accumulate in this phase upon heat shock
370 (Frottin et al., 2019). Thus, it is likely that CHIP embedded in GC associates with
371 aggregated proteins, which affects its mobility.

372
373 What is the role of CHIP in the nucleolus? We hypothesized that in collaboration with
374 HSP70, CHIP might serve as a ubiquitin ligase or co-chaperone that regulates
375 ubiquitination or substrate reassembly to aid in the regeneration process. To revise
376 this, we focused on recovering a specifically modified luciferase that contained a
377 nucleus-targeting sequence to facilitate its accumulation in the nucleolus upon heat
378 shock. The effect of CHIP on luciferase status during heat shock and recovery but not
379 in association with the nucleolus was previously studied *in vitro* and *in cellulo*, showing
380 ambiguous results. CHIP can maintain denatured luciferase in a state capable of
381 folding and ubiquitinate it *in vitro* (Rosser et al., 2007). Moreover, heat shock may
382 enhance CHIP chaperone activity and its ability to suppress luciferase aggregation *in*
383 *vitro* (Rosser et al., 2007). In heat-stressed HEK293 cells, it was demonstrated that
384 CHIP overexpression protected luciferase activity and did not cause its increased
385 degradation. CHIP was also able to specifically interact with thermally denatured
386 luciferase rather than with the refolded one (Rosser et al., 2007). In fibroblasts, CHIP
387 overexpression did not affect luciferase degradation after heat shock and during
388 recovery but increased its HSP70-dependent reassembly and protected it from heat-
389 induced insolubility (Kampinga et al., 2003). On the other hand, there are also
390 conflicting data indicating that CHIP overexpression can inhibit the renaturation of
391 denatured luciferase in Cos-7 cells and reduce HSP70 or HSP70:HSP40-mediated
392 luciferase folding *in vitro* (Ballinger et al., 1999; Marques et al., 2006). Overall, the
393 effect of CHIP on luciferase status is indisputable but may depend on multiple factors.

394
395 Our results suggest that CHIP abundance in nucleoli slows the rate of luciferase
396 recovery from heat shock. Knowing that there is no increased aggregation of CHIP in
397 nucleoli, we consider it unlikely that the presence of CHIP imposes additional stress
398 on this organelle. Furthermore, noting that the CHIP HSP70-binding deficient K30A

399 mutant does not significantly delay luciferase refolding despite its presence in nucleoli,
400 we propose that CHIP controls this process via interaction with HSP70. Regulation of
401 HSP70 by CHIP in the nucleolus may involve a reduction in the affinity of this
402 chaperone for substrates, as shown previously (Ballinger et al., 1999; Stankiewicz et
403 al., 2010). Also, CHIP may affect the rate of ATP hydrolysis by HSP70 (Stankiewicz et
404 al., 2010), which may also shape the condensation state in the nucleolus and thus the
405 environment for the recovery processes (Yewdall et al., 2021). Noteworthy, HSP70
406 may inhibit CHIP ubiquitination activity (Narayan et al., 2015; Das et al., 2021),
407 resulting in a functional co-regulation of these proteins to select the optimal heat stress
408 response in the nucleolus. We would also like to point out that we observed significantly
409 higher CHIP levels in the nucleoli of heat-stressed HeLa EGFP-CHIP or MCF7 cells
410 than in the luciferase-expressing HEK293T cells upon CHIP overexpression. We
411 speculate that these particular cancer cells may more intensively utilize CHIP to
412 manage proteostasis in the nucleus.

413
414 The role of CHIP ubiquitination activity in protein recovery in the nucleolus remains
415 elusive and thus requires further study, perhaps by using other inactive CHIP variants
416 and investigating their effects on ubiquitination and recovery of specific endogenous
417 proteins. However, our FRAP analysis and data obtained from prolonged heat shock
418 revealed altered dynamics and pro-aggregation characteristics of the catalytically
419 inactive CHIP H260Q mutant, which we hypothesize may indirectly affect nucleolar
420 protein regeneration. It would be interesting to investigate whether other CHIP inactive
421 variants, also pathogenic, show greater sensitivity to heat stress, affecting nucleoli
422 regeneration.

423
424 The mechanisms that trigger CHIP clearance from the nucleolus during regeneration
425 are also unclear. We observed that the signals indicating the presence of luciferase
426 and CHIP in the nucleolus decreased with similar dynamics, suggesting that some
427 level of recovery must be achieved before CHIP is released. Recent proteomic data
428 revealed proteins associated with NPM1 in recovering from heat shock VER-treated
429 HEK293T cells, showing a persistent impairment of nucleolar regeneration in the
430 presence of the inhibitor (Frottin et al., 2019). Intriguingly, CHIP was not identified in
431 this study, although it was detected in nucleoli after heat shock when VER was not
432 added. This may suggest that CHIP acts specifically and targets selected nucleolar
433 proteins during the regeneration process. When we treated cells with VER throughout
434 the heat shock and recovery, we encountered increased CHIP levels in HeLa EGFP-
435 CHIP and MCF7 cells. This further supports our hypothesis on the functional cross-talk
436 between CHIP and HSP70, and HSP70 inhibition-dependent CHIP response to
437 alterations in the recovery efficiency.

438
439 We also found that cells can clear nucleolar luciferase foci even after prolonged heat
440 shock, and this process is also affected by CHIP overexpression. Frottin et al. showed
441 that prolonged heat shock overloads nucleolar capacity in the same cells and may be
442 responsible for aberrant phase behavior associated with the danger of irreversible
443 protein aggregation (Frottin et al., 2019). The process was entirely reversible in our
444 hands, suggesting that cells adapted to stress. It is important to note that in our
445 experimental scheme, cells were exposed to 42°C heat shock instead of 43°C.
446 Therefore, it would be interesting to test if we balanced around the “point of no return”
447 where we came across a temperature-dependent differential cell capability to manage
448 stress. In conclusion, we predict that the presence of CHIP in nucleoli may provide a

449 mechanism for selective and regulated recovery of proteins, which may be relevant for
450 cell survival during proteotoxic stress.

451

452 **FIGURE LEGENDS**

453

454 **Fig. 1 CHIP translocates to nucleoli in heat-stressed cells**

455

456 A) Scheme of the heat shock assay. In most experiments, cells were exposed to
457 heat stress at 42°C for 90 min (120 min for HEK293T cells) and transferred to
458 37°C for 2 h recovery.

459 B) Overexpressed EGFP-CHIP in HeLa Flp-In cells (HeLa EGFP-CHIP cells)
460 shows nucleolar localization after heat shock (white arrowheads). Cells were
461 imaged live before heat shock (control), immediately after heat shock (HS), and
462 post-heat shock recovery (Rec). Scale bar represents 10 μ m.

463 C) Endogenous CHIP can migrate to nucleoli upon heat shock. Confocal images
464 of HeLa Flp-In cells after immunofluorescent staining for CHIP (green) and
465 NPM1 (red) in control, heat-stressed (HS), and recovered (Rec) cells. Scale bar
466 represents 10 μ m.

467 D) Western blot after HeLa Flp-In cell fractionation to cytoplasmic (Cyt),
468 nucleoplasmic (Nuc), and nucleolar fractions showing CHIP and HSP70
469 accumulation in nucleoli after heat shock. Fractions purity was evaluated by
470 detecting α -tubulin (cytoplasm), lamin B1 (nucleoplasm), and fibrillarin, FBL
471 (nucleoli).

472 E) Representative confocal images of HeLa Flp-In cells transiently expressing the
473 EGFP-CHIP K30A show weaker translocation of this co-chaperone mutant to
474 nucleoli upon heat shock (HS). Scale bar represents 10 μ m.

475

476

477 **Fig. 2 HSP70-dependent localization of CHIP in nucleoli**

478

479 A) CHIP colocalizes with HSP70 upon heat shock. Confocal images (with
480 Airyscan) of HeLa EGFP-CHIP cells after immunostaining for HSP70 (red).
481 Scale bar represents 5 μ m.

482 B) HSP70 recruits CHIP to nucleoli during heat shock. Quantification of mean
483 CHIP intensity in nucleoli during 90 min heat shock and 2 h-recovery in HeLa
484 EGFP-CHIP cells upon HSP70 knockdown. Data are means of three
485 independent experiments. Error bars show SD. Statistical significance was
486 determined using a two-way ANOVA followed by Tukey's multiple comparison
487 test ($***P < 0.001$, $**P < 0.01$, $*P < 0.05$).

488 C) Quantification of the percentage of cells with CHIP present in nucleoli during
489 heat shock and 2 h-recovery in HeLa EGFP-CHIP cells upon HSP70
490 knockdown. Data are means of three independent experiments. Error bars show
491 SD. Statistical significance was determined using a two-way ANOVA followed
492 by Tukey's multiple comparison test ($****P < 0.0001$).

493 D) HSP70 inhibition by VER does not affect CHIP migration to nucleoli during heat
494 shock but blocks its release during recovery. HeLa EGFP-CHIP cells were
495 treated with 40 μ M VER before heat shock, and CHIP intensity was measured
496 in nucleoli in control cells during heat shock and 2 h-recovery. Data are means
497 of three independent experiments. Error bars show SD. Statistical significance

- 498 was determined using a two-way ANOVA followed by Tukey's multiple
499 comparison test ($****P < 0.0001$, $***P < 0.001$, $**P < 0.01$, $ns P > 0.05$).
- 500 E) HSP70 inhibition by VER during post-heat shock recovery only slightly affects
501 CHIP clearance from nucleoli. HeLa EGFP-CHIP cells were exposed to 90 min
502 heat shock and treated with 40 μ M VER before transferring them for the 2 h-
503 recovery. CHIP intensity was measured in nucleoli in control cells during heat
504 shock and recovery. Data are means of four independent experiments. Error
505 bars show SD. Statistical significance was determined using two-tailed unpaired
506 t-tests for pairwise comparisons ($****P < 0.0001$, $***P < 0.001$, $*P < 0.05$).
- 507 F) CHIP maintains high mobility in the nucleolus upon heat shock. Analysis of
508 FRAP kinetics of EGFP-CHIP in the nucleolus of untreated (green) or treated
509 with 40 μ M VER (red) HeLa EGFP-CHIP cells during heat shock. Points show
510 mean values from 9 or 19 nucleoli analysis from untreated or VER-treated cells,
511 respectively. Error bars show SD (grey for untreated cells, pink for VER-treated
512 cells). Fitting curves are shown in black.
- 513 G) CHIP dynamics quantification in HeLa EGFP-CHIP cells during post-heat shock
514 recovery in the presence of 40 μ M VER. FRAP kinetics were measured in 15
515 nucleoli after 1 h-recovery. Error bars show SD. A fitting curve is shown in black.
- 516

517 **Fig. 3 Nucleolar CHIP colocalizes with the NPM1-containing granular component**
518 **(GC) phase**

519

- 520 A) Confocal images (with Airyscan) of HeLa EGFP-CHIP cells immunostained for
521 NPM1. Cells were exposed to the following conditions: heat shock, heat shock
522 in the presence of 40 μ M VER, or treated with VER throughout heat shock and
523 recovery (HS + Rec + VER), followed by immunostaining. Scale bar represents
524 5 μ m.
- 525 B) Confocal images (with Airyscan) of HeLa EGFP-CHIP cells immunostained for
526 FBL. Cells were exposed to the following conditions: heat shock, heat shock in
527 the presence of 40 μ M VER, or treated with VER throughout heat shock and
528 recovery (HS + Rec+ VER), followed by immunostaining. Scale bar represents
529 5 μ m.
- 530 C) Quantification of the degree of colocalization of EGFP-CHIP and NPM1 and
531 EGFP-CHIP and FBL using Pearson's correlation coefficient. Violin plots show
532 the data from 31 to 70 nucleoli analyzed per condition. Two-tailed unpaired t-
533 tests were used for comparisons. Statistical significance level $****P < 0.0001$.
- 534

535 **Fig. 4 CHIP import to nucleoli is not induced by nucleolar stress *per se***

536

- 537 A) Actinomycin D (Act D) does not induce CHIP migration to nucleoli in HeLa
538 EGFP-CHIP cells. Cells were treated with 0.05 μ g/ml Act D for 30 min or 2 h
539 and imaged live. Representative confocal images of cells after 2 h Act D
540 treatment. Scale bar represents 10 μ m.
- 541 B) Pretreatment with 0.05 μ g/ml Act D before heat shock does not affect CHIP
542 migration to nucleoli during heat shock but impairs its exit. Quantification of
543 mean CHIP intensity in nucleoli after 90 min heat shock and 2 h-recovery in
544 HeLa EGFP-CHIP cells pretreated with Act D for 30 min or 2 h. Data are means
545 of three independent experiments. Error bars show SD. Statistical significance
546 was determined using a one-way ANOVA followed by Dunnett's multiple
547 comparison tests ($****P < 0.0001$, $*P < 0.05$).

- 548 C) Pretreatment with 0.05 $\mu\text{g/ml}$ Act D before heat shock does not affect CHIP
549 migration to nucleoli during heat shock but impairs its exit. Quantification of the
550 percentage of cells with CHIP present in nucleoli after 90 min heat shock and
551 2 h-recovery in HeLa EGFP-CHIP cells pretreated with Act D for 30 min or 2 h.
552 Data are means of three independent experiments. Error bars show SD.
553 Statistical significance was determined using a one-way ANOVA followed by
554 Dunnett's multiple comparison tests (** $P < 0.01$).
- 555 D) Treatment with Act D prior to heat shock alters CHIP distribution in nucleoli.
556 HeLa EGFP-CHIP cells were pretreated with 0.05 $\mu\text{g/ml}$ Act D for 2 h before
557 heat shock, followed by immunostaining for NPM1 and confocal imaging.
558 Representative images and their magnified views of cells after heat shock (HS)
559 vs. cells treated with Act D before heat shock (Act D + HS) are shown.
560 Scale bars represent 10 μm or 5 μm (magnified views).

561
562 **Fig. 5 CHIP activity promotes its dynamics in the nucleolus**

- 563
- 564 A) Heat shock and post-heat shock recovery do not affect CHIP ubiquitination
565 activity. Western blot depicting CHIP auto-ubiquitination following *in vitro*
566 ubiquitination assay. HEK EGFP-CHIP cells were exposed to 90 min heat shock
567 and 1 h-recovery. After treatment, cell lysates were used for *in vitro*
568 ubiquitination assay. The assays performed in the presence of the lysate without
569 other components in the reaction mixture (lysate) or without the addition of
570 ubiquitin (- Ub) were served as negative controls. Protein samples were
571 resolved via SDS-PAGE and immunoblotted with anti-GFP and GAPDH
572 (loading control) antibodies.
- 573 B) Inactive CHIP H260Q mutant can migrate to nucleoli during heat shock.
574 Representative confocal images of HeLa Flp-In cells transiently expressing the
575 EGFP-CHIP H260Q mutant in control conditions and after heat shock (HS). The
576 arrowhead points at the nucleolus containing mutant CHIP. Scale bar
577 represents 10 μm .
- 578 C) The CHIP H260Q mutant shows reduced mobility in nucleoli. FRAP kinetics of
579 CHIP H260Q compared to CHIP WT in nucleoli of heat-shocked cells. The
580 mutant CHIP mobility was measured in HeLa Flp-In cells after transient
581 expression of EGFP-CHIP H260Q. FRAP analysis of EGFP-CHIP WT was
582 originally shown in Fig. 2F and is displayed here again for comparison with CHIP
583 H260Q recovery curves. CHIP H260Q FRAP kinetics were measured in 12
584 nucleoli. Error bars show SD. Fitting curves are shown in black.
- 585 D) Confocal images of nucleolar EGFP-CHIP WT (upper panel) and EGFP-CHIP
586 H260Q mutant (bottom panel), showing movie frames before bleaching and 0,
587 10, 30, and 50 s after bleaching in the FRAP assays. The bleached region of
588 interest is marked with circles. Differences in CHIP intensities are displayed in
589 pseudo-colored images using Green Fire Blue LUT (look-up table) in ImageJ
590 software. Scale bars represent 2 μm .
- 591 E) Large droplet-like structures are preferentially formed by the CHIP H260Q
592 mutant in nucleoli of cells exposed to prolonged heat shock. Representative
593 confocal images of HeLa Flp-In cells transiently expressing mCherry, mCherry-
594 CHIP WT, and mCherry-CHIP H260Q mutant and treated with overnight heat
595 shock. Arrowheads point at CHIP intra-nucleolar assemblies. Scale bar
596 represents 5 μm .

- 597 F) Quantification of the percentage of nucleoli with CHIP droplet-like structures
598 after overnight heat shock in cells transiently expressing CHIP WT or the CHIP
599 H260Q mutant. Data were collected from two independent experiments: 38 and
600 43 nucleoli with CHIP WT and H260Q mutant, respectively.
- 601 G) Boxplot of the mean intensities of CHIP droplet-like structures inside nucleoli of
602 cells transiently expressing CHIP WT or the CHIP H260Q mutant after overnight
603 heat shock. Note that if there were several droplets inside nucleoli, the intensity
604 was measured for the brightest one. 17 CHIP WT and 38 CHIP H260Q droplets
605 across two biological repeats were analyzed. The line in the middle of the box
606 is plotted at the median. Whiskers extend from the 5th to 95th percentiles. Two-
607 tailed Welch's t-test was used for comparison, $**P < 0.01$.
- 608 H) Quantification of the diameters of CHIP droplet-like structures inside nucleoli of
609 cells transiently expressing CHIP WT or the CHIP H260Q mutant after overnight
610 heat shock. Note that if there were several droplets inside nucleoli, the
611 measurement was performed for the biggest one. 17 CHIP WT and 38 CHIP
612 H260Q droplets across two biological repeats were analyzed. The line in the
613 middle of the box is plotted at the median. Whiskers extend from the 5th to 95th
614 percentiles. For comparison two-tailed Mann-Whitney test was used, $*P < 0.05$.
- 615 I) Boxplot of the areas of CHIP droplet-like structures inside nucleoli of cells
616 transiently expressing CHIP WT or the CHIP H260Q mutant after overnight heat
617 shock. Note that if there were several droplets inside nucleoli, the measurement
618 was performed for the biggest one. 17 CHIP WT and 38 CHIP H260Q droplets
619 across two biological repeats were analyzed. The line in the middle of the box
620 is plotted at the median. Whiskers extend from the 5th to 95th percentiles. For
621 comparison two-tailed Mann-Whitney test was used, $*P < 0.05$.
- 622

623 **Fig. 6 CHIP overexpression affects the nucleolar luciferase recovery**

624

- 625 A) Nucleolar CHIP colocalizes with luciferase after heat shock. HEK293T cells
626 stably expressing luciferase were transfected with mCherry-CHIP and subject
627 to heat shock for 2 h. After treatment cells were immunostained for NPM1 and
628 imaged using the Airyscanning technique. Arrowheads show overlapped
629 signals of luciferase (green), mCherry-CHIP (red) and NPM1 (purple). Scale
630 bars represent 5 μm .
- 631 B) Luciferase foci dissolution during post-heat shock recovery is slower in cells
632 expressing CHIP WT or CHIP H260Q but not in cells expressing CHIP K30A.
633 HEK293T cells permanently expressing luciferase were transfected with vectors
634 encoding for mCherry, mCherry-CHIP WT, mCherry-CHIP H260Q and
635 mCherry-CHIP K30A. 24 h after transfection cells were subject to 2 h heat shock
636 and the recovery was monitored for 6 h afterward. Cells were imaged live using
637 confocal microscopy. Luciferase foci were counted in untransfected and
638 mCherry-expressing cells (control groups) and cells expressing the appropriate
639 CHIP variant. The percentage of cells with nucleolar luciferase foci was
640 determined for each condition. Data were normalized to correct for cell
641 percentage differences after heat shock and in control conditions between
642 experimental groups and are expressed as the ratio of % cells with luciferase
643 foci at the specific time point to % cells with luciferase foci upon heat shock
644 calculated for a given group. Data are means of three independent experiments.
645 Error bars represent SD. For statistical comparison a two-way ANOVA with post
646 hoc Tukey's test was used ($***P < 0.001$, $**P < 0.01$, $*P < 0.05$).

- 647 C) CHIP is redistributed to nucleoli during heat shock and leaves this compartment
648 during recovery. During recovery, the CHIP H260Q mutant's exit from nucleoli
649 is the slowest compared to CHIP WT and CHIP K30A. HEK293T cells
650 permanently expressing luciferase were transfected with vectors encoding for
651 mCherry-CHIP WT, mCherry-CHIP H260Q and mCherry-CHIP K30A and
652 treated with 2 h heat shock followed by 6 h recovery. Cells during treatments
653 were imaged live using confocal microscopy. Images were analyzed for the
654 mean mCherry intensities as a proxy for CHIP concentrations in the nucleoli and
655 nuclei, and the relative intensities were quantified. Data are means of three
656 independent experiments. Error bars represent SD. For statistical comparison
657 a two-way ANOVA with post hoc Tukey's test was used ($**P < 0.01$, $ns P >$
658 0.05).
- 659 D) CHIP WT and CHIP H260Q overexpression disrupt the regeneration rate of
660 luciferase in nucleoli. HEK293T cells permanently expressing luciferase were
661 transfected with vectors encoding for mCherry, mCherry-CHIP WT, mCherry-
662 CHIP H260Q, and mCherry-CHIP K30A and treated with 2 h heat shock
663 followed by 6 h recovery. Confocal images of live cells were taken after indicated
664 time points and images were analyzed for mean intensities of GFP-tagged
665 luciferase in whole nucleoli relative to nuclei. Data are means of three
666 independent experiments. Error bars represent SD. For statistical comparison
667 a two-way ANOVA with post hoc Tukey's test was used ($****P < 0.0001$, $***P <$
668 0.001 , $ns P > 0.05$).

670 **Fig. 7 HSP70 inhibition aggravates the negative effect of CHIP on luciferase**
671 **regeneration**

- 673 A) Cells overexpressing CHIP WT show mildly impaired nucleolar luciferase
674 regeneration in the presence of VER. HEK293T cells stably expressing
675 luciferase were transfected with the vectors encoding for mCherry-CHIP
676 variants. 24 h after transfection cells were subject to 2 h heat shock and
677 recovery. Prior to the recovery period cells were treated with 40 μ M VER or
678 recovery was initiated without the compound treatment. The plot shows the
679 quantification of nucleolar luciferase foci in untransfected cells and cells
680 expressing CHIP WT imaged by confocal microscopy. Data are means of three
681 independent experiments and are expressed as a % of total cell counts. Error
682 bars represent SD. For statistical comparison, a two-way ANOVA with post hoc
683 Tukey's test was used ($**P < 0.01$, $*P < 0.05$).
- 684 B) Overexpression of the CHIP K30A or CHIP H260Q mutants cause more
685 disruptive effects on luciferase regeneration in the presence of VER. HEK293T
686 cells stably expressing luciferase were transfected with the vectors encoding for
687 mCherry-CHIP variants. Prior to the recovery period, cells were treated with
688 40 μ M VER or recovery was initiated without the compound treatment. The plot
689 shows the quantification of nucleolar luciferase foci in cells expressing CHIP
690 K30A and CHIP H260Q imaged by confocal microscopy. Data are means of
691 three independent experiments and are expressed as a % of total cell counts.
692 Error bars represent SD. For statistical comparison a two-way ANOVA followed
693 by Tukey's multiple comparison test was used ($***P < 0.001$, $**P < 0.01$,
694 $*P < 0.05$).

695
696

697 **SUPPLEMENTARY FIGURE LEGENDS**

698

699

Figure S1. CHIP localizes to nucleoli specifically during heat shock

700

701 A) A simplified scheme of genomic elements after targeted integration of the

702 EGFP-CHIP transgene into HeLa Flp-In T-REx and 293 Flp-In T-REx cell lines

703 (modified from (Szczeny et al., 2018)). Generated cells are resistant to

704 hygromycin B but sensitive to zeocin selection antibiotic. The EGFP-CHIP

705 expression is repressed by the activity of the repressor protein TetR and

706 induced by the addition of tetracycline to the culture medium.

707 B) Other tested stressors do not induce CHIP migration to nucleoli. HEK EGFP-

708 CHIP cells were exposed to various stressors: 90 min heat shock at 42°C,

709 50 µM sodium arsenite, 100 nM thapsigargin, 0.6 M sorbitol and 2 mg/ml

710 puromycin for 2 h. Confocal images and their magnified views of cells after each

711 stress are shown. The arrowhead shows CHIP in the nucleolus of the heat-

712 stressed cell. Scale bars represent 10 µm or 5 µm (magnified views).

713 C) Confocal images of MCF7 cells transiently expressing EGFP-CHIP. Cells

714 treated with heat shock show CHIP nucleolar accumulation. The lack of Hoechst

715 333412 staining recognizes nucleoli. A scale bar represents 5 µm.

716 D) Confocal images of MCF7 cells after immunostaining for CHIP (green) and

717 NPM1 (red). Nuclei (blue) are labelled with DAPI. Images show representative

718 cells during control conditions, after 90 min heat shock and after heat shock and

719 recovery in the presence of the 40 µM VER inhibitor (HS + Rec + VER). Nucleoli

720 are indicated by arrowheads and are also marked with dashed circles. A scale

721 bar represents 5 µm.

722 E) Quantification of relative mean CHIP intensities: from nucleoli vs. nuclei in

723 MCF7 cells from confocal images. Selected images are shown in Figure S1D.

724 Cells were treated with heat shock and 2 h recovery without or with VER, which

725 was applied either for complete treatment (HS + Rec + VER) or only during

726 recovery (Rec + VER). Control cells also received 40 µM VER for 2 h. Plotted

727 data show individual experiments. For statistical comparison a one-way ANOVA

728 followed by Tukey's multiple comparison test was used (** $P < 0.01$, * $P < 0.05$).

729

730 **Figure S2. Validation of HSP70 knockdown efficiency in HeLa EGFP-CHIP cells**

731

732 A) Confocal images of HeLa EGFP-CHIP cells after HSP70 knockdown *via* siRNA.

733 To control for the effects of siRNA delivery, nontargeting siRNA was used

734 (sineg). 72 h after siRNA transfection, control and heat-shocked cells were

735 immunostained for HSP70 (red) and the nuclei were stained with DAPI. Scale

736 bars represent 10 µm.

737

738 **Figure S3. Actinomycin D (Act D) alters nucleolar morphology resulting in**
739 **prolonged sequestration of CHIP in nucleoli during recovery from heat shock**

740

741 A) Confocal images of HeLa EGFP-CHIP cells after immunostaining for NPM1 (left

742 panel) and FBL (right panel). Indicated cells were pretreated with 0.05 µg/ml

743 Act D for 2 h followed by immunostaining and confocal imaging. Arrowheads

744 point at FBL nucleolar caps formed in the presence of Act D. Scale bars

745 represent 10 µm.

- 746 B) Analysis of changes in nucleolar morphology upon Act D treatment. HeLa
747 EGFP-CHIP cells were treated with 0.05 $\mu\text{g/ml}$ Act D for 30 min and 2 h alone
748 or followed by 90 min heat shock. Next, cells were fixed and immunostained for
749 NPM1 and FBL nucleolar proteins. The mean nucleolar area, circularity (based
750 on NPM1 signal) and percentage of nuclei with nucleolar caps (based on FBL
751 signal) were quantified. Data are means of two (area, circularity) and three
752 (nucleolar caps) independent experiments. Error bars represent SD. For
753 statistical comparison a one-way ANOVA followed by Dunnett's multiple
754 comparisons test was used ($***P < 0.001$, $**P < 0.01$).
- 755 C) Confocal images of HeLa EGFP-CHIP cells after the 2 h-recovery from heat
756 shock (Recovery) or pretreated with 0.05 $\mu\text{g/ml}$ Act D for 2 h before the heat
757 shock and recovery periods (Act D + Recovery). After treatment, cells were
758 imaged live. Arrowheads indicate nucleolar CHIP in Act D- treated cells. Scale
759 bar represents 10 μm .
- 760

761 **Figure S4. CHIP overexpression affects the nucleolar luciferase recovery**

762

- 763 A) HEK293T cells permanently expressing luciferase were transfected with vectors
764 encoding for mCherry, mCherry-CHIP WT, mCherry-CHIP H260Q and
765 mCherry-CHIP K30A. 24 h after transfection cells were subject to 2 h heat shock
766 and the recovery was monitored for 6 h afterward. Cells were imaged live using
767 confocal microscopy. Luciferase foci were counted in untransfected and
768 mCherry-expressing cells (control groups) and cells expressing the appropriate
769 CHIP variant. The percentage of cells with nucleolar luciferase foci was
770 determined for each condition. Data are means of three independent
771 experiments. Error bars represent SD. For statistical comparison a two-way
772 ANOVA with post hoc Tukey's test was used ($****P < 0.0001$, $***P < 0.001$, $**P$
773 < 0.01 , $*P < 0.05$).
- 774 B) HEK293T cells permanently expressing luciferase were transfected with vectors
775 encoding for mCherry, mCherry-CHIP WT, mCherry-CHIP H260Q, and
776 mCherry-CHIP K30A. Transfection was performed with 0.2 μg plasmids per well
777 of the 8-well chamber. 24 h after transfection cells were subject to 2 h-heat
778 shock followed by 2 h-recovery. Images of live cells at the indicated time were
779 taken using confocal microscopy. Luciferase foci were counted in untransfected
780 and mCherry-expressing cells (control groups) and cells expressing the
781 appropriate CHIP variant. The percentage of cells with nucleolar luciferase foci
782 was determined for each condition. Data normalization was performed as
783 described in Fig. 6B. Data are means of three independent experiments. Error
784 bars represent SD. For statistical comparison, a two-way ANOVA with post hoc
785 Tukey's test was used ($***P < 0.001$, $**P < 0.01$, $*P < 0.05$).
- 786

787 **Figure S5. During prolonged heat shock, luciferase recovery in nucleoli is**
788 **affected by CHIP WT and CHIP H260Q overexpression**

789

- 790 A) HEK293T cells permanently expressing luciferase were transfected with vectors
791 encoding for mCherry, mCherry-CHIP WT, mCherry-CHIP H260Q and
792 mCherry-CHIP K30A and treated with 6 h heat shock. Every 2 h cells were
793 imaged live using confocal microscopy. Images were analyzed for mean
794 intensities of GFP-tagged luciferase in whole nucleoli relative to nuclei. Data are
795 means of three independent experiments. Error bars represent SD. For

796 statistical comparison a two-way ANOVA with post hoc Tukey's test was used
797 ($****P < 0.0001$, $***P < 0.001$, $ns P > 0.05$).

798 B) HEK293T cells permanently expressing luciferase were transfected with vectors
799 encoding for mCherry, mCherry-CHIP WT, mCherry-CHIP H260Q and
800 mCherry-CHIP K30A and treated with 6 h heat shock. During treatments cells
801 were imaged by confocal microscopy. Luciferase foci were counted in
802 untransfected and mCherry-expressing cells (control groups) and cells
803 expressing the appropriate CHIP variant. The percentages of total cell counts
804 were quantified for each condition. Data normalization was performed as
805 described in Fig. 6B. Data are means of three independent experiments. Error
806 bars represent SD. For statistical comparison, a two-way ANOVA with post hoc
807 Tukey's test was used ($***P < 0.001$, $ns P > 0.05$).

808 C) CHIP WT and H260Q show sustained sequestration into nucleoli during
809 prolonged heat stress. HEK293T cells permanently expressing luciferase were
810 transfected with vectors encoding for mCherry-CHIP WT, mCherry-CHIP
811 H260Q and mCherry-CHIP K30A and treated with 6 h heat shock. Every 2 h
812 intervals, confocal images of live cells were taken to measure CHIP intensities
813 in nucleoli and nuclei, and the relative intensities were quantified. Data are
814 means of three independent experiments. Error bars represent SD. For
815 statistical comparison a two-way ANOVA with post hoc Tukey's test was used
816 ($****P < 0.0001$, $***P < 0.001$, $**P < 0.01$, $*P < 0.05$, $ns P > 0.05$).

817

818

819 MATERIALS AND METHODS

820

821 METHODS

822

823 Cell culture

824

825 HeLa Flp-In T-REx, HEK293 Flp-In T-REx (a kind gift from Dr. R. Szczesny), MCF7 (a
826 kind gift from Prof. A. Zylicz), HeLa EGFP-CHIP, HEK EGFP-CHIP, and HEK293T NLS
827 LG cells (stably expressing luciferase; a kind gift from Dr. M.S. Hipp) were cultured in
828 Dulbecco's Modified Eagle's Medium (D6429, Sigma) supplemented with 10% heat-
829 inactivated fetal bovine serum (Sigma) and 1% antibiotic - antimycotic (Gibco) at 37°C
830 with 5% CO₂ in a humidified incubator. To maintain stable cell lines, HeLa EGFP-CHIP
831 and HEK EGFP-CHIP cells were supplemented with blasticidin (10 µg/ml) (ant-bl-1,
832 Invivogen) and hygromycin B (50 µg/ml) (10687010, Thermo Fisher Scientific), while
833 293T NLS LG cells were supplemented with G418 (100 µg/ml) (10131035, Gibco). For
834 the experiment, the EGFP-CHIP expression in HeLa EGFP-CHIP and HEK EGFP-
835 CHIP cells was induced by adding tetracycline to the medium (25 ng/ml) upon plating.
836 Where indicated, to induce heat shock, cells were transferred to another humidified
837 incubator set at 42°C. For the recovery, cells were transferred back to 37°C. For
838 passaging and experiments, cells were dissociated from the plate with trypsin (Trypsin-
839 EDTA 0.25%, Sigma). Cells were tested for mycoplasma using a PCR-based assay.

840

841 Poly-L-lysine coating

842

843 HEK293T cells were grown on cover glasses or 8 well-chambered slides (Ibidi) coated
844 with Poly-L-lysine solution (P4707, Sigma). The coating was performed for 1 h at 37°C,
845 followed by two washes in sterile PBS and drying under a laminar flow hood.

846 Tetracycline preparation

847
848 Tetracycline was prepared according to an established protocol (Szczeny et al.,
849 2018). Briefly, tetracycline was added to 96% ethanol at the 5 mg/ml concentration.
850 The solution was rotated for 30 min at room temperature and incubated overnight at
851 -20°C. The next day the rotation was repeated for 30 min. Afterward, it was filtered
852 through the 0.22 µm syringe filter and diluted with ethanol to the final concentration of
853 100 µg/ml. The solution was stored at -20°C.

854 Plasmid construction

855
856
857 Vectors: pKK-EGFP-TEV and pKK-mCherry-TEV were a kind gift from Dr. R.
858 Szczeny.

859 The sequence and ligation independent cloning (SLIC) method was used to construct
860 mCherry-CHIP, mCherry-CHIP H260Q, mCherry-CHIP K30A, EGFP-CHIP, EGFP-
861 CHIP H260Q plasmids. The parental vectors (pKK-EGFP-TEV and pKK-mCherry-
862 TEV) were linearized with BshTI i NheI enzymes. For SLIC cloning, linearized vectors
863 were mixed with PCR-amplified human CHIP sequence and treated with T4 DNA
864 polymerase, followed by bacterial transformation. The following primers were used for
865 CHIP sequence amplification:

866 **hCHIP forward:**

867 GGATCCgaaaacctgtacttccaaggaACCGGTATGAAGGGCAAGGAGGAGAAG

868 **hCHIP reverse:**

869 GATATCaccctgaaaatacaaatctcGCTAGCTCAGTAGTCCTCCACCCAGC

870
871
872 To insert H260Q mutation into the CHIP sequence, two PCR reactions were carried
873 out using the following primers:

874
875 The 1st amplicon:

876 **hCHIP forward:**

877 GGATCCgaaaacctgtacttccaaggaACCGGTATGAAGGGCAAGGAGGAGAAG

878 **r1:** CACGCTGCAGcTGCTCCTCGATGTCC

880
881 The 2nd amplicon:

882 **f1:** GGACATCGAGGAGCAgCTGCAGCGTG

883 **hCHIP reverse:**

884 GATATCaccctgaaaatacaaatctcGCTAGCTCAGTAGTCCTCCACCCAGC

885
886
887 Afterward, splice-PCR was used to assemble both fragments.

888
889 Sequence validation was performed using restriction enzymes (BamHI and EcoRV)
890 and sequencing with the following primers:

891
892 **FRTTO_For** tgacctccatagaagacacc

893 **FRTTO_Rev** aactagaaggcacagtgcgag

894 **EGFP_F** catggctctgctggagtgcg

895 **CHIP_For** atgaagggaaggaggagaag

896 To generate EGFP-CHIP K30A plasmid, Q5 Site-Directed Mutagenesis Kit
897 (E0554S, New England Biolabs) was used with the following primers:

898

899 **F-hCHIP K30A:** GCAGGAGCTCgcGGAGCAGGGCAATC

900 **R-hCHIP K30A:** GCGCTCGGGCTCTTCTCG

901

902 Stable cell line generation

903

904 HeLa Flp-In T-REx and HEK293 Flp-In T-REx cells were grown on 6-well plates. For
905 stable cell line generation, the cells were co-transfected with 1 µg pOG44 (a kind gift
906 from Dr. R. Szczeny) and 0.8 µg EGFP-CHIP plasmid using Mirus reagents: 2 ul
907 TransIT-293 (MIR 2700, Mirus) for transfection of HEK293 Flp-In T-REx cells and 2 ul
908 Trans-IT-HeLa and 1.3 ul Monster (MIR 2900, Mirus) for HeLa Flp-In T-REx cells. The
909 day following transfection cells were treated with selection antibiotics: 10 µg/ml
910 blasticidin (Invivogen) and 50 µg/ml hygromycin B (Thermo Fisher Scientific). The
911 treatment continued for a month.

912

913 Cell transfection

914

915 Transient transfections were performed using Lipofectamine 2000 (Invitrogen)
916 according to the manufacturer's guidelines. Cells seeded on 8 well-chambered slides
917 (Ibidi) were transfected with 0.5 µg plasmid per well. Cells seeded for VER-155008
918 treatment were transfected with 0.2 µg plasmid. Transfections were carried out a day
919 before imaging.

920

921 HSP70 knockdown

922

923 HeLa EGFP-CHIP cells were seeded on 35 mm imaging dishes (Ibidi). The following
924 day cells were co-transfected with 75 pmols HSP70 siRNAs (IDs 145248 and 6965,
925 Thermo Fisher Scientific) using 9 µl Lipofectamine RNAiMAX reagent (Invitrogen) in
926 Opti-MEM Reduced Serum Medium. The medium was exchanged after 48 h post-
927 transfection. Silencing lasted 72 h.

928

929 Actinomycin D and VER-155008 treatments

930

931 Cells were treated with 0.05 µg/ml Actinomycin D (Act D) (1229, Tocris) dissolved in
932 DMSO in a complete medium for 0.5 or 2 h at 37°C. Then the cells were exposed to
933 90 min heat shock at 42°C and 120 min of recovery at 37°C. The cells were fixed for
934 immunofluorescence, or live cells were imaged using confocal microscopy.

935

936 VER-155008 (SML0271, Sigma) dissolved in DMSO was added to the complete
937 medium at the final concentration of 40 µM. HEK293T and MCF7 cells were treated
938 with VER-155008 before the heat shock, while HeLa EGFP-CHIP cells were pretreated
939 with VER-155008 for 2 h before the heat shock. All cell lines were treated with VER-
940 155008 immediately after the heat shock for recovery. Cells were fixed for
941 immunofluorescence, or live cells were imaged using confocal microscopy.

942

943

944 Immunofluorescence

945
946 Cells were fixed with 4% (para)formaldehyde (28906, Pierce) in PBS for 10 min at room
947 temperature before washing 3 times with PBS for 5 min. The cells were permeabilized
948 for 10 min with Triton X-100 0.1% (v/v) in PBS at room temperature. Samples were
949 incubated in a blocking buffer (either 2% bovine serum albumin BSA, 1.5% goat serum,
950 0.1% Triton X-100 in PBS, or 1% BSA in PBS) for 10 min at room temperature. Primary
951 antibodies were applied in a blocking buffer and incubated overnight at 4°C.
952 Appropriate fluorescent secondary antibodies at a dilution of 1:500 were applied after
953 PBS washes for 60 min at room temperature in PBS. Samples were mounted using
954 the Vectashield antifade mounting medium with DAPI (Vector Laboratories).

955 956 Primary antibodies:

- 957 ▪ CHIP (1:250) rabbit [EPR4447] (ab134064) Abcam
- 958 ▪ NPM1 (1:250) mouse (32-5200) Invitrogen
- 959 ▪ FBL (1:400) rabbit (2639S) Cell Signaling Technology
- 960 ▪ HSP70 (1:250) mouse (SMC-100) StressMarq Biosciences

961 962 Secondary antibodies:

963 Goat Alexa 647 anti-mouse (A21235, Invitrogen), goat Alexa 568 anti-mouse (A11031,
964 Invitrogen), goat Alexa 647 anti-rabbit (A21245, Invitrogen).

965 966 Image acquisition

967
968 Confocal microscopy was performed on the ZEISS LSM800 confocal laser scanning
969 microscope (Carl Zeiss Microscopy) using 63x/1.4 NA or 40x/1.3 NA oil immersion
970 objectives. Images show single optical sections. Within each experiment, images were
971 acquired using identical acquisition settings. For colocalization studies, imaging was
972 carried out with Airyscan.

973 974 Image analysis

975
976 ImageJ software (<https://imagej.nih.gov/ij/index.html>) (Schneider et al., 2012) was
977 used for image analysis in most experiments except for MCF7 immunostaining. In
978 HeLa EGFP-CHIP cells, nucleoli were manually selected, and the CHIP (EGFP)
979 intensity (mean gray value) was calculated. For colocalization studies, the JaCoP
980 plugin was used (Bolte and Cordelières, 2006). The image background was corrected
981 using the rolling ball algorithm (rolling ball=150). Thresholds of the green and red
982 channels were selected manually and maintained in every image.

983 984 Analysis of the fluorescence intensity ratio - nucleolus: nucleus in HEK293T cells

985
986 Nucleoli were manually located using the Hoechst 33342 channel. Relative luciferase
987 or CHIP concentrations in nucleoli/nuclei were calculated based on GFP or mCherry
988 intensities, respectively, in each compartment in 50 cells per condition across three
989 biological repeats.

990
991
992
993

994 Quantification of nucleolar luciferase foci in HEK293T cells

995
996 Luciferase foci were counted in 47-142 cells (66-301 cells for the experiments with
997 VER-155008) per time point and condition across 3 biological repeats.

998 999 Analysis of CHIP ratio in MCF7 cells

1000
1001 Image analysis was conducted with a customized CellProfiler 4.2.1. (Carpenter et al.,
1002 2006; Stirling et al., 2021) pipeline. In short, nuclei and nucleoli objects were
1003 segmented from DAPI and NPM1 channels, respectively, using the three-class Otsu
1004 thresholding method, excluding objects touching the image's border. Next, the nuclei
1005 objects were masked by nucleoli objects, thus creating the third class of objects –
1006 masked nuclei, consisting solely of nucleoplasm without nucleoli. The relationship of
1007 each nucleolus object to its parent nucleus object was assigned using the
1008 RelateObjects module. Finally, CHIP intensity was calculated from the CHIP channel
1009 for both masked nuclei and nucleoli objects and exported together with the relationship
1010 information to CSV files. For each repetition of the experiment, the ratio of each child
1011 nucleolus/parent masked nucleus mean intensities was calculated. Nucleoli without
1012 assigned parent nucleus (parent ID 0) were discarded from the analysis.

1013 1014 FRAP

1015
1016 Cells used in FRAP studies were cultured on 35-mm imaging dishes (Ibidi). FRAP
1017 experiments were performed on ZEISS LSM800 confocal laser scanning microscope
1018 equipped with the 40x/1.3 NA oil immersion objective. A circular region of interest of
1019 the constant size was selected within nucleoli, and bleaching was carried out with
1020 100% laser power of the 488 nm laser line. Fluorescence intensity was recorded for
1021 up to 3 min at a frame interval of 0.5 s. FRAP movies were analyzed using
1022 FRAPAnalyser (<https://github.com/ssgpers/FRAPAnalyser>). Fluorescence intensity
1023 was corrected for background fluorescence and photobleaching. Recovery curves
1024 were fitted with a single exponential recovery.

1025 1026 Nucleoli isolation

1027
1028 Cells grown on 100 mm tissue culture dishes were harvested on ice. The isolation of
1029 nucleoli was performed according to the previously described protocol with some
1030 modifications (Andersen et al., 2002). The old medium was discarded, and the cells
1031 were washed 1x with 4 ml of ice-cold PBS. Cells were harvested on ice in cold PBS.
1032 The cells were washed 1x with ice-cold PBS at 220 x g at 4°C. After the PBS wash,
1033 the cells were resuspended in 5 ml of Buffer A (10 mM HEPES pH 7.9, 10 mM KCl,
1034 1.5 mM MgCl₂, 0.5 mM DTT, 1x Complete protease inhibitor cocktail (Roche)) and
1035 incubated on ice for 5 min. The cells were homogenized with a pre-cooled 1 ml Dounce
1036 homogenizer (Wheaton) on ice 10x using a tight pestle. The homogenized cells were
1037 centrifuged at 220 x g for 5 min at 4°C. The supernatant was collected as the
1038 cytoplasmic fraction. The pellet was resuspended with 3 ml S1 solution (0.25 M
1039 sucrose, 10 mM MgCl₂, 1x Complete protease inhibitor cocktail (Roche)) by pipetting
1040 up and down. The resuspended pellet was layered carefully over 3 ml of S2 solution
1041 (0.35 M sucrose, 0.5 mM MgCl₂, 1x Complete protease inhibitor cocktail (Roche)) and
1042 centrifuged at 1430 x g for 5 min at 4°C. The pellet was resuspended with 3 ml of S2
1043 solution by pipetting up and down. The nuclear suspension was sonicated on the ice

1044 at 50% power 11x, each time for 10 s and 10 s of rest on ice (Sonica VCX130 with a
1045 ¼ inch tip). The sonicated sample was layered over 3 ml of S3 solution
1046 (0.88 M sucrose, 0.5 mM MgCl₂, 1x Complete protease inhibitor cocktail (Roche)) in a
1047 new Falcon tube and centrifuged at 3000 × g for 10 min at 4°C. The supernatant was
1048 collected as the nucleoplasm fraction. The pellet was resuspended with 500 µl of S2
1049 solution and centrifuged at 1430 × g for 5 min at 4°C. The nucleoli were resuspended
1050 in 500 µL of S2 solution and stored at –80°C as nucleoli fractions.

1051

1052 Estimation of the protein concentration and Western blotting

1053

1054 The protein concentration was estimated using the BCA protein assay kit (23225,
1055 Thermo Scientific). Protein samples in SDS-loading dye (reducing) were run in 10%
1056 acrylamide gels in a running buffer (25 mM Tris, 190 mM glycine, 0.1% SDS) at 90 V
1057 (stacking gel) and 150 V (separating gel). The wet transfer was done at a constant
1058 400 mA for 1 h at 4°C in a transfer buffer (25 mM Tris, 190 mM glycine, 20% methanol,
1059 pH 8.3). Blots were blocked with 5% skimmed milk in TBST (50 mM Tris, 150 mM
1060 NaCl, 0.1% Tween 20, pH 7.6) for 1 h at room temperature and incubated overnight
1061 with primary antibodies prepared in 5% skimmed milk in TBST at 4°C. The blots were
1062 then washed three times with TBST for 10 min each wash. Finally, the blots were
1063 incubated with horseradish peroxidase-linked secondary antibodies (1:10000)
1064 prepared in 5% skimmed milk in TBST for 1 h at room temperature. Imaging was
1065 performed using a ChemiDoc™ Imaging System (Bio-Rad).

1066

1067 Antibodies:

- 1068 ▪ CHIP (1: 1000) rabbit [EPR4447] (ab134064) Abcam
- 1069 ▪ FBL (1: 500) rabbit (2639S) Cell Signaling Technology
- 1070 ▪ Alpha-tubulin (1: 1000) mouse (32-2500) Invitrogen
- 1071 ▪ Lamin B1 (1: 1000) mouse (33-2000) Invitrogen
- 1072 ▪ HSP70 (1: 500) mouse (SMC-100) StressMarq Biosciences

1073

1074 In vitro ubiquitination assay

1075

1076 The reactions were run at 37°C for 90 min using 60 µM Ubiquitin (Boston Biochem) in
1077 the presence of 100 nM E1 (UBE1, Boston Biochem), 0.6 µM E2 (Boston Biochem),
1078 E3 ligase reaction buffer (Boston Biochem), and ATP in 25 µl reaction mixture. 2 µl cell
1079 lysates served as a source of the E3 ligase CHIP (cells were lysed in Cell lysis buffer
1080 (9803, Cell Signaling Technology). After reactions, protein samples were mixed with
1081 the SDS-loading dye and boiled for Western blot analysis.

1082

1083 Statistical analysis

1084

1085 Data were plotted and analyzed with the GraphPad Prism 9 software. P-values were
1086 calculated using a two-way or one way ANOVA followed by multiple comparisons tests.
1087 Two-tailed unpaired t-test or Mann-Whitney test were used to compare differences
1088 between two independent groups. In the figures, * = p< 0.05, ** = p< 0.01, *** = p<
1089 0.001, **** = p< 0.0001.

1090

1091

1092

1093

1094 **ACKNOWLEDGEMENTS**

1095
1096 We thank the Genome Engineering Unit of the International Institute of Molecular and
1097 Cell Biology in Warsaw for generating DNA constructs. We thank the Microscopy and
1098 Cytometry Facility of the International Institute of Molecular and Cell Biology in Warsaw
1099 for assistance with the confocal microscopy. We thank Aleksandra Szybińska for
1100 optimizing the HSP70 knockdown in HeLa EGFP-CHIP cells. We thank members of
1101 the Pokrzywa laboratory for discussions and comments on the manuscript.

1102 **FUNDING**

1103
1104
1105 L.B., K.K. and W.P. were supported by the Foundation for Polish Science, co-financed
1106 by the European Union under the European Regional Development Fund (grant
1107 POIR.04.04.00-00-5EAB/18-00) M.P. was supported by the Norwegian Financial
1108 Mechanism 2014-2021 and operated by the Polish National Science Center under the
1109 project contract no UMO-2019/34/H/NZ3/00691.

1110 **CONFLICT OF INTEREST**

1111
1112
1113 The authors declare that the research was conducted without any commercial or
1114 financial relationships that could be construed as a potential conflict of interest.

1115 **AUTHOR CONTRIBUTIONS**

1116
1117
1118 Contributions of individual authors based on the [CRediT](#) (Contributor Roles
1119 Taxonomy).

1120
1121 **Malgorzata Piechota:** Conceptualization; Data curation; Formal analysis;
1122 Methodology; Investigation; Validation; Visualization; Supervision; Validation; Writing-
1123 original draft; Writing-review & editing. **Lilla Biriczova:** Formal analysis; Investigation;
1124 Methodology; Visualization; Writing-review & editing. **Konrad Kowalski:** Formal
1125 analysis; Investigation; Methodology; Visualization; Writing-review & editing. **Natalia**
1126 **A. Szulc:** Formal analysis; Writing-review & editing. **Wojciech**
1127 **Pokrzywa:** Conceptualization; Data curation; Formal analysis; Funding acquisition;
1128 Project administration; Resources; Supervision; Validation; Writing-original draft;
1129 Writing-review & editing.

1130 **REFERENCES**

1131
1132
1133 Alberti, S., and Carra, S. (2019). Nucleolus: A Liquid Droplet Compartment for
1134 Misbehaving Proteins. *Curr Biol* 29(19), R930-r932. doi:
1135 10.1016/j.cub.2019.08.013.
1136 Andersen, J.S., Lyon, C.E., Fox, A.H., Leung, A.K., Lam, Y.W., Steen, H., et al. (2002).
1137 Directed proteomic analysis of the human nucleolus. *Curr Biol* 12(1), 1-11. doi:
1138 10.1016/s0960-9822(01)00650-9.
1139 Audas, T.E., Jacob, M.D., and Lee, S. (2012). Immobilization of proteins in the
1140 nucleolus by ribosomal intergenic spacer noncoding RNA. *Mol Cell* 45(2), 147-
1141 157. doi: 10.1016/j.molcel.2011.12.012.

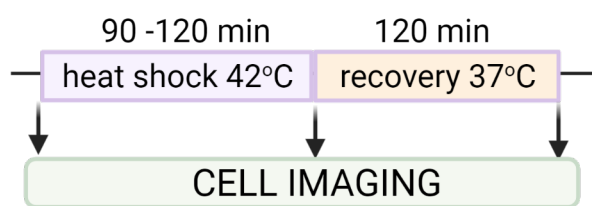
- 1142 Azkanaz, M., Rodríguez López, A., de Boer, B., Huiting, W., Angrand, P.O., Vellenga,
1143 E., et al. (2019). Protein quality control in the nucleolus safeguards recovery of
1144 epigenetic regulators after heat shock. *Elife* 8. doi: 10.7554/eLife.45205.
- 1145 Ballinger, C.A., Connell, P., Wu, Y., Hu, Z., Thompson, L.J., Yin, L.Y., et al. (1999).
1146 Identification of CHIP, a novel tetratricopeptide repeat-containing protein that
1147 interacts with heat shock proteins and negatively regulates chaperone
1148 functions. *Mol Cell Biol* 19(6), 4535-4545. doi: 10.1128/mcb.19.6.4535.
- 1149 Biggiogera, M., Bürki, K., Kaufmann, S.H., Shaper, J.H., Gas, N., Amalric, F., et al.
1150 (1990). Nucleolar distribution of proteins B23 and nucleolin in mouse
1151 preimplantation embryos as visualized by immunoelectron microscopy.
1152 *Development* 110(4), 1263-1270. doi: 10.1242/dev.110.4.1263.
- 1153 Bolte, S., and Cordelières, F.P. (2006). A guided tour into subcellular colocalization
1154 analysis in light microscopy. *J Microsc* 224(Pt 3), 213-232. doi: 10.1111/j.1365-
1155 2818.2006.01706.x.
- 1156 Buetow, L., and Huang, D.T. (2016). Structural insights into the catalysis and regulation
1157 of E3 ubiquitin ligases. *Nat Rev Mol Cell Biol* 17(10), 626-642. doi:
1158 10.1038/nrm.2016.91.
- 1159 Carpenter, A.E., Jones, T.R., Lamprecht, M.R., Clarke, C., Kang, I.H., Friman, O., et
1160 al. (2006). CellProfiler: image analysis software for identifying and quantifying
1161 cell phenotypes. *Genome Biol* 7(10), R100. doi: 10.1186/gb-2006-7-10-r100.
- 1162 Cerqueira, A.V., and Lemos, B. (2019). Ribosomal DNA and the Nucleolus as
1163 Keystones of Nuclear Architecture, Organization, and Function. *Trends Genet*
1164 35(10), 710-723. doi: 10.1016/j.tig.2019.07.011.
- 1165 Dai, Q., Zhang, C., Wu, Y., McDonough, H., Whaley, R.A., Godfrey, V., et al. (2003).
1166 CHIP activates HSF1 and confers protection against apoptosis and cellular
1167 stress. *Embo j* 22(20), 5446-5458. doi: 10.1093/emboj/cdg529.
- 1168 Das, A., Thapa, P., Santiago, U., Shanmugam, N., Banasiak, K., Dabrowska, K., et al.
1169 (2021). Heterotypic Assembly Mechanism Regulates CHIP E3 Ligase Activity.
1170 *bioRxiv*, 2021.2008.2020.457118. doi: 10.1101/2021.08.20.457118.
- 1171 Demand, J., Alberti, S., Patterson, C., and Höhfeld, J. (2001). Cooperation of a
1172 ubiquitin domain protein and an E3 ubiquitin ligase during
1173 chaperone/proteasome coupling. *Curr Biol* 11(20), 1569-1577. doi:
1174 10.1016/s0960-9822(01)00487-0.
- 1175 Feric, M., Vaidya, N., Harmon, T.S., Mitrea, D.M., Zhu, L., Richardson, T.M., et al.
1176 (2016). Coexisting Liquid Phases Underlie Nucleolar Subcompartments. *Cell*
1177 165(7), 1686-1697. doi: 10.1016/j.cell.2016.04.047.
- 1178 Frottin, F., Schueder, F., Tiwary, S., Gupta, R., Körner, R., Schlichthaerle, T., et al.
1179 (2019). The nucleolus functions as a phase-separated protein quality control
1180 compartment. *Science* 365(6451), 342-347. doi: 10.1126/science.aaw9157.
- 1181 Hatakeyama, S., Yada, M., Matsumoto, M., Ishida, N., and Nakayama, K.I. (2001). U
1182 box proteins as a new family of ubiquitin-protein ligases. *J Biol Chem* 276(35),
1183 33111-33120. doi: 10.1074/jbc.M102755200.
- 1184 Huang, S. (2002). Building an efficient factory: where is pre-rRNA synthesized in the
1185 nucleolus? *J Cell Biol* 157(5), 739-741. doi: 10.1083/jcb.200204159.
- 1186 Jiang, J., Ballinger, C.A., Wu, Y., Dai, Q., Cyr, D.M., Höhfeld, J., et al. (2001). CHIP is
1187 a U-box-dependent E3 ubiquitin ligase: identification of Hsc70 as a target for
1188 ubiquitylation. *J Biol Chem* 276(46), 42938-42944. doi:
1189 10.1074/jbc.M101968200.
- 1190 Jordan, E.G. (1984). Nucleolar nomenclature. *J Cell Sci* 67, 217-220. doi:
1191 10.1242/jcs.67.1.217.

- 1192 Joshi, V., Amanullah, A., Upadhyay, A., Mishra, R., Kumar, A., and Mishra, A. (2016).
1193 A Decade of Boon or Burden: What Has the CHIP Ever Done for Cellular Protein
1194 Quality Control Mechanism Implicated in Neurodegeneration and Aging? *Front*
1195 *Mol Neurosci* 9, 93. doi: 10.3389/fnmol.2016.00093.
- 1196 Kampinga, H.H., Kanon, B., Salomons, F.A., Kabakov, A.E., and Patterson, C. (2003).
1197 Overexpression of the cochaperone CHIP enhances Hsp70-dependent folding
1198 activity in mammalian cells. *Mol Cell Biol* 23(14), 4948-4958. doi:
1199 10.1128/MCB.23.14.4948-4958.2003.
- 1200 Komander, D. (2009). The emerging complexity of protein ubiquitination. *Biochem Soc*
1201 *Trans* 37(Pt 5), 937-953. doi: 10.1042/bst0370937.
- 1202 Kozakai, Y., Kamada, R., Furuta, J., Kiyota, Y., Chuman, Y., and Sakaguchi, K. (2016).
1203 PPM1D controls nucleolar formation by up-regulating phosphorylation of
1204 nucleophosmin. *Sci Rep* 6, 33272. doi: 10.1038/srep33272.
- 1205 Krüger, T., Zentgraf, H., and Scheer, U. (2007). Intranucleolar sites of ribosome
1206 biogenesis defined by the localization of early binding ribosomal proteins. *J Cell*
1207 *Biol* 177(4), 573-578. doi: 10.1083/jcb.200612048.
- 1208 Lafontaine, D.L.J., Riback, J.A., Bascetin, R., and Brangwynne, C.P. (2021). The
1209 nucleolus as a multiphase liquid condensate. *Nat Rev Mol Cell Biol* 22(3), 165-
1210 182. doi: 10.1038/s41580-020-0272-6.
- 1211 Latonen, L., Moore, H.M., Bai, B., Jäämaa, S., and Laiho, M. (2011). Proteasome
1212 inhibitors induce nucleolar aggregation of proteasome target proteins and
1213 polyadenylated RNA by altering ubiquitin availability. *Oncogene* 30(7), 790-805.
1214 doi: 10.1038/onc.2010.469.
- 1215 Lindström, M.S., Jurada, D., Bursac, S., Orsolich, I., Bartek, J., and Volarevic, S. (2018).
1216 Nucleolus as an emerging hub in maintenance of genome stability and cancer
1217 pathogenesis. *Oncogene* 37(18), 2351-2366. doi: 10.1038/s41388-017-0121-z.
- 1218 Marques, C., Guo, W., Pereira, P., Taylor, A., Patterson, C., Evans, P.C., et al. (2006).
1219 The triage of damaged proteins: degradation by the ubiquitin-proteasome
1220 pathway or repair by molecular chaperones. *Faseb j* 20(6), 741-743. doi:
1221 10.1096/fj.05-5080fje.
- 1222 Meacham, G.C., Patterson, C., Zhang, W., Younger, J.M., and Cyr, D.M. (2001). The
1223 Hsc70 co-chaperone CHIP targets immature CFTR for proteasomal
1224 degradation. *Nat Cell Biol* 3(1), 100-105. doi: 10.1038/35050509.
- 1225 Mediani, L., Guillén-Boixet, J., Vinet, J., Franzmann, T.M., Bigi, I., Mateju, D., et al.
1226 (2019). Defective ribosomal products challenge nuclear function by impairing
1227 nuclear condensate dynamics and immobilizing ubiquitin. *Embo j* 38(15),
1228 e101341. doi: 10.15252/emboj.2018101341.
- 1229 Mekhail, K., Khacho, M., Carrigan, A., Hache, R.R., Gunaratnam, L., and Lee, S.
1230 (2005). Regulation of ubiquitin ligase dynamics by the nucleolus. *J Cell Biol*
1231 170(5), 733-744. doi: 10.1083/jcb.200506030.
- 1232 Mitrea, D.M., Cika, J.A., Stanley, C.B., Nourse, A., Onuchic, P.L., Banerjee, P.R., et
1233 al. (2018). Self-interaction of NPM1 modulates multiple mechanisms of liquid-
1234 liquid phase separation. *Nat Commun* 9(1), 842. doi: 10.1038/s41467-018-
1235 03255-3.
- 1236 Murata, S., Minami, Y., Minami, M., Chiba, T., and Tanaka, K. (2001). CHIP is a
1237 chaperone-dependent E3 ligase that ubiquitylates unfolded protein. *EMBO Rep*
1238 2(12), 1133-1138. doi: 10.1093/embo-reports/kve246.
- 1239 Narayan, V., Landré, V., Ning, J., Hernychova, L., Muller, P., Verma, C., et al. (2015).
1240 Protein-Protein Interactions Modulate the Docking-Dependent E3-Ubiquitin

- 1241 Ligase Activity of Carboxy-Terminus of Hsc70-Interacting Protein (CHIP). *Mol*
1242 *Cell Proteomics* 14(11), 2973-2987. doi: 10.1074/mcp.M115.051169.
- 1243 Nollen, E.A., Salomons, F.A., Brunsting, J.F., van der Want, J.J., Sibon, O.C., and
1244 Kampinga, H.H. (2001). Dynamic changes in the localization of thermally
1245 unfolded nuclear proteins associated with chaperone-dependent protection.
1246 *Proc Natl Acad Sci U S A* 98(21), 12038-12043. doi: 10.1073/pnas.201112398.
- 1247 Pelham, H., Lewis, M., and Lindquist, S. (1984). Expression of a Drosophila heat shock
1248 protein in mammalian cells: transient association with nucleoli after heat shock.
1249 *Philos Trans R Soc Lond B Biol Sci* 307(1132), 301-307. doi:
1250 10.1098/rstb.1984.0131.
- 1251 Pelham, H.R. (1984). Hsp70 accelerates the recovery of nucleolar morphology after
1252 heat shock. *Embo j* 3(13), 3095-3100. doi: 10.1002/j.1460-
1253 2075.1984.tb02264.x.
- 1254 Petrucelli, L., Dickson, D., Kehoe, K., Taylor, J., Snyder, H., Grover, A., et al. (2004).
1255 CHIP and Hsp70 regulate tau ubiquitination, degradation and aggregation. *Hum*
1256 *Mol Genet* 13(7), 703-714. doi: 10.1093/hmg/ddh083.
- 1257 Qian, S.B., McDonough, H., Boellmann, F., Cyr, D.M., and Patterson, C. (2006). CHIP-
1258 mediated stress recovery by sequential ubiquitination of substrates and Hsp70.
1259 *Nature* 440(7083), 551-555. doi: 10.1038/nature04600.
- 1260 Reynolds, R.C., Montgomery, P.O., and Hughes, B. (1964). NUCLEOLAR "CAPS"
1261 PRODUCED BY ACTINOMYCIN D. *Cancer Res* 24, 1269-1277.
- 1262 Riback, J.A., Zhu, L., Ferrolino, M.C., Tolbert, M., Mitrea, D.M., Sanders, D.W., et al.
1263 (2020). Composition-dependent thermodynamics of intracellular phase
1264 separation. *Nature* 581(7807), 209-214. doi: 10.1038/s41586-020-2256-2.
- 1265 Rosser, M.F., Washburn, E., Muchowski, P.J., Patterson, C., and Cyr, D.M. (2007).
1266 Chaperone functions of the E3 ubiquitin ligase CHIP. *J Biol Chem* 282(31),
1267 22267-22277. doi: 10.1074/jbc.M700513200.
- 1268 Scheer, U., and Hock, R. (1999). Structure and function of the nucleolus. *Curr Opin*
1269 *Cell Biol* 11(3), 385-390. doi: 10.1016/s0955-0674(99)80054-4.
- 1270 Schlecht, R., Scholz, S.R., Dahmen, H., Wegener, A., Sirrenberg, C., Musil, D., et al.
1271 (2013). Functional analysis of Hsp70 inhibitors. *PLoS One* 8(11), e78443. doi:
1272 10.1371/journal.pone.0078443.
- 1273 Schneider, C.A., Rasband, W.S., and Eliceiri, K.W. (2012). NIH Image to ImageJ: 25
1274 years of image analysis. *Nat Methods* 9(7), 671-675. doi: 10.1038/nmeth.2089.
- 1275 Shav-Tal, Y., Blechman, J., Darzacq, X., Montagna, C., Dye, B.T., Patton, J.G., et al.
1276 (2005). Dynamic sorting of nuclear components into distinct nucleolar caps
1277 during transcriptional inhibition. *Mol Biol Cell* 16(5), 2395-2413. doi:
1278 10.1091/mbc.e04-11-0992.
- 1279 Shimura, H., Schwartz, D., Gygi, S.P., and Kosik, K.S. (2004). CHIP-Hsc70 complex
1280 ubiquitinates phosphorylated tau and enhances cell survival. *J Biol Chem*
1281 279(6), 4869-4876. doi: 10.1074/jbc.M305838200.
- 1282 Smirnov, E., Borkovec, J., Kováčik, L., Svidenská, S., Schröfel, A., Skalníková, M., et
1283 al. (2014). Separation of replication and transcription domains in nucleoli. *J*
1284 *Struct Biol* 188(3), 259-266. doi: 10.1016/j.jsb.2014.10.001.
- 1285 Stankiewicz, M., Nikolay, R., Rybin, V., and Mayer, M.P. (2010). CHIP participates in
1286 protein triage decisions by preferentially ubiquitinating Hsp70-bound substrates.
1287 *Febs j* 277(16), 3353-3367. doi: 10.1111/j.1742-4658.2010.07737.x.
- 1288 Stirling, D.R., Swain-Bowden, M.J., Lucas, A.M., Carpenter, A.E., Cimini, B.A., and
1289 Goodman, A. (2021). CellProfiler 4: improvements in speed, utility and usability.
1290 *BMC Bioinformatics* 22(1), 433. doi: 10.1186/s12859-021-04344-9.

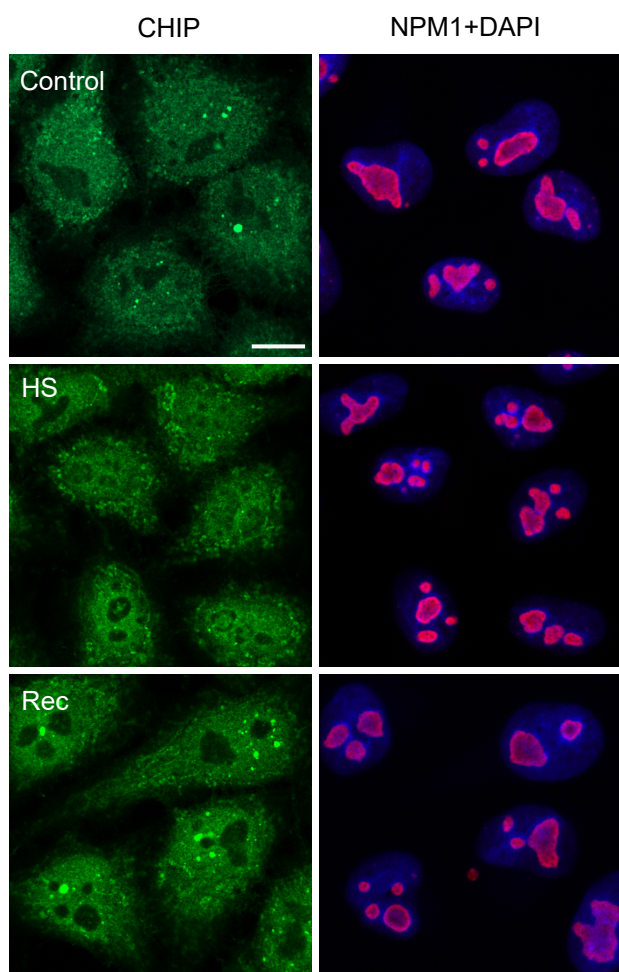
- 1291 Szaflarski, W., Leśniczak-Staszak, M., Sowiński, M., Ojha, S., Aulas, A., Dave, D., et
1292 al. (2022). Early rRNA processing is a stress-dependent regulatory event whose
1293 inhibition maintains nucleolar integrity. *Nucleic Acids Res* 50(2), 1033-1051. doi:
1294 10.1093/nar/gkab1231.
- 1295 Szczesny, R.J., Kowalska, K., Klosowska-Kosicka, K., Chlebowski, A., Owczarek,
1296 E.P., Warkocki, Z., et al. (2018). Versatile approach for functional analysis of
1297 human proteins and efficient stable cell line generation using FLP-mediated
1298 recombination system. *PLoS One* 13(3), e0194887. doi:
1299 10.1371/journal.pone.0194887.
- 1300 Tateishi, Y., Kawabe, Y., Chiba, T., Murata, S., Ichikawa, K., Murayama, A., et al.
1301 (2004). Ligand-dependent switching of ubiquitin-proteasome pathways for
1302 estrogen receptor. *Embo j* 23(24), 4813-4823. doi: 10.1038/sj.emboj.7600472.
- 1303 Wang, M., Bokros, M., Theodoridis, P.R., and Lee, S. (2019). Nucleolar Sequestration:
1304 Remodeling Nucleoli Into Amyloid Bodies. *Front Genet* 10, 1179. doi:
1305 10.3389/fgene.2019.01179.
- 1306 Welch, W.J., and Feramisco, J.R. (1984). Nuclear and nucleolar localization of the
1307 72,000-dalton heat shock protein in heat-shocked mammalian cells. *J Biol*
1308 *Chem* 259(7), 4501-4513.
- 1309 Welch, W.J., and Suhan, J.P. (1986). Cellular and biochemical events in mammalian
1310 cells during and after recovery from physiological stress. *J Cell Biol* 103(5),
1311 2035-2052. doi: 10.1083/jcb.103.5.2035.
- 1312 Wu, X., and Hammer, J.A. (2021). ZEISS Airyscan: Optimizing Usage for Fast, Gentle,
1313 Super-Resolution Imaging. *Methods Mol Biol* 2304, 111-130. doi: 10.1007/978-
1314 1-0716-1402-0_5.
- 1315 Yang, K., Wang, M., Zhao, Y., Sun, X., Yang, Y., Li, X., et al. (2016). A redox
1316 mechanism underlying nucleolar stress sensing by nucleophosmin. *Nat*
1317 *Commun* 7, 13599. doi: 10.1038/ncomms13599.
- 1318 Yewdall, N.A., André, A.A.M., van Haren, M.H.I., Nelissen, F.H.T., Jonker, A., and
1319 Spruijt, E. (2021). ATP:Mg²⁺ shapes condensate properties of rRNA-NPM1 *in*
1320 *vitro* nucleolus model and its partitioning of ribosomes. *bioRxiv*,
1321 2021.2012.2022.473778. doi: 10.1101/2021.12.22.473778.
- 1322 Younger, J.M., Ren, H.Y., Chen, L., Fan, C.Y., Fields, A., Patterson, C., et al. (2004).
1323 A foldable CFTR{Delta}F508 biogenic intermediate accumulates upon inhibition
1324 of the Hsc70-CHIP E3 ubiquitin ligase. *J Cell Biol* 167(6), 1075-1085. doi:
1325 10.1083/jcb.200410065.
- 1326

A

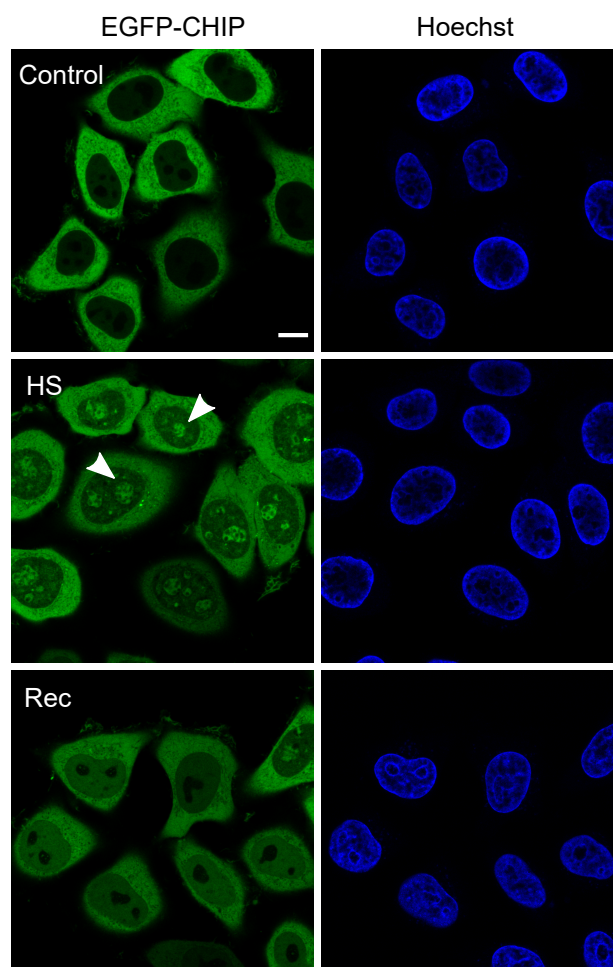


Created with BioRender.com

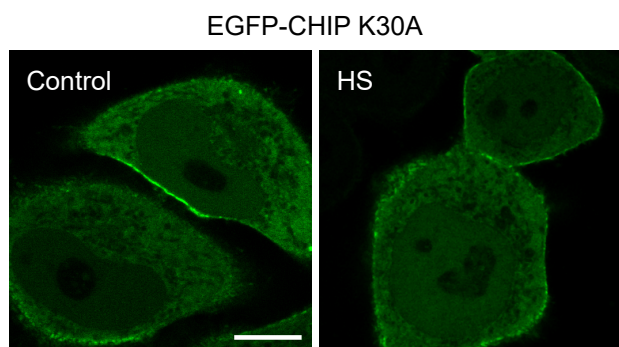
C



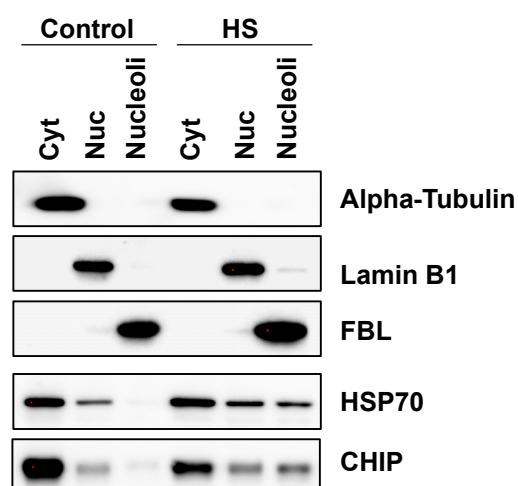
B

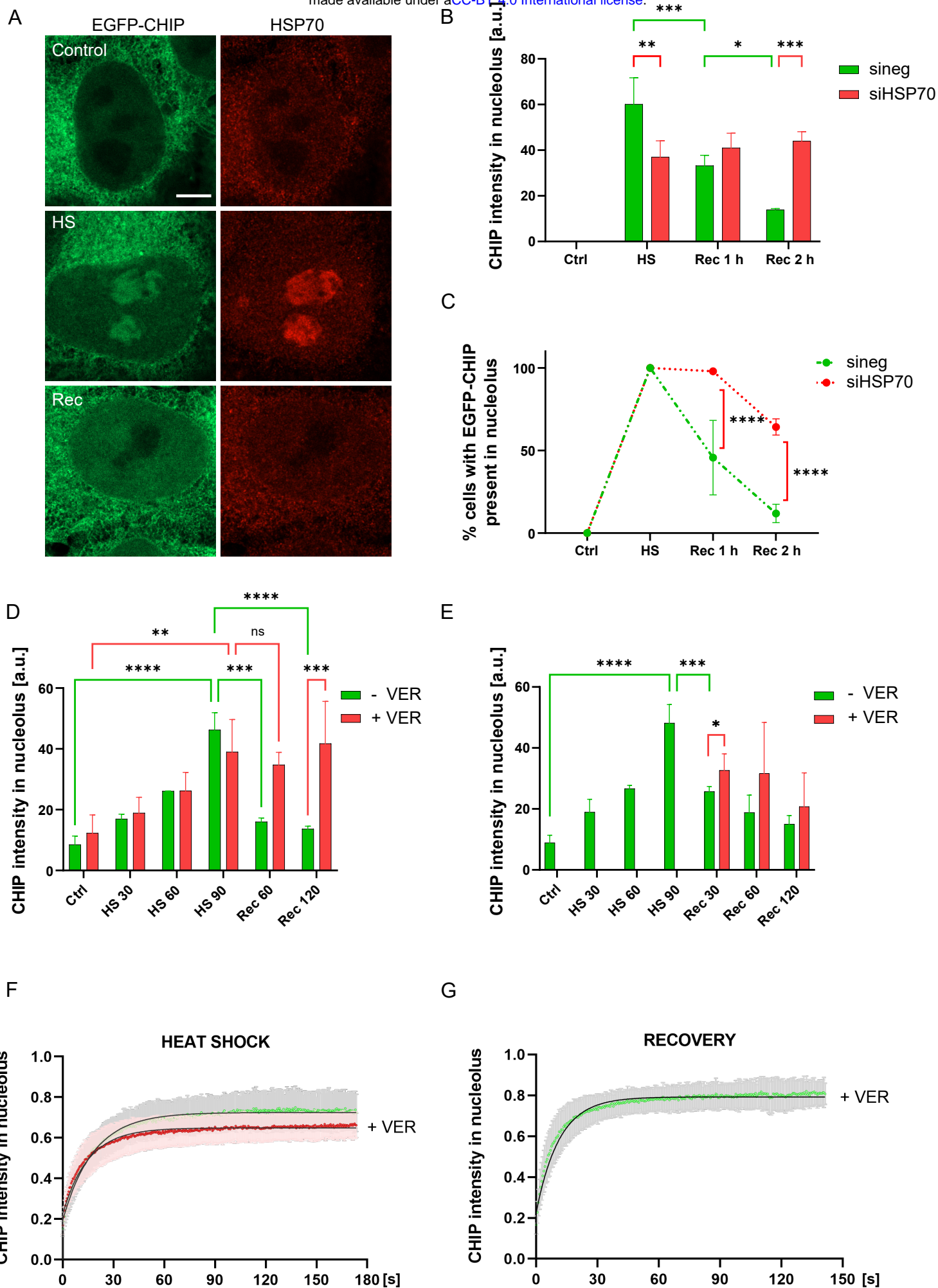


E

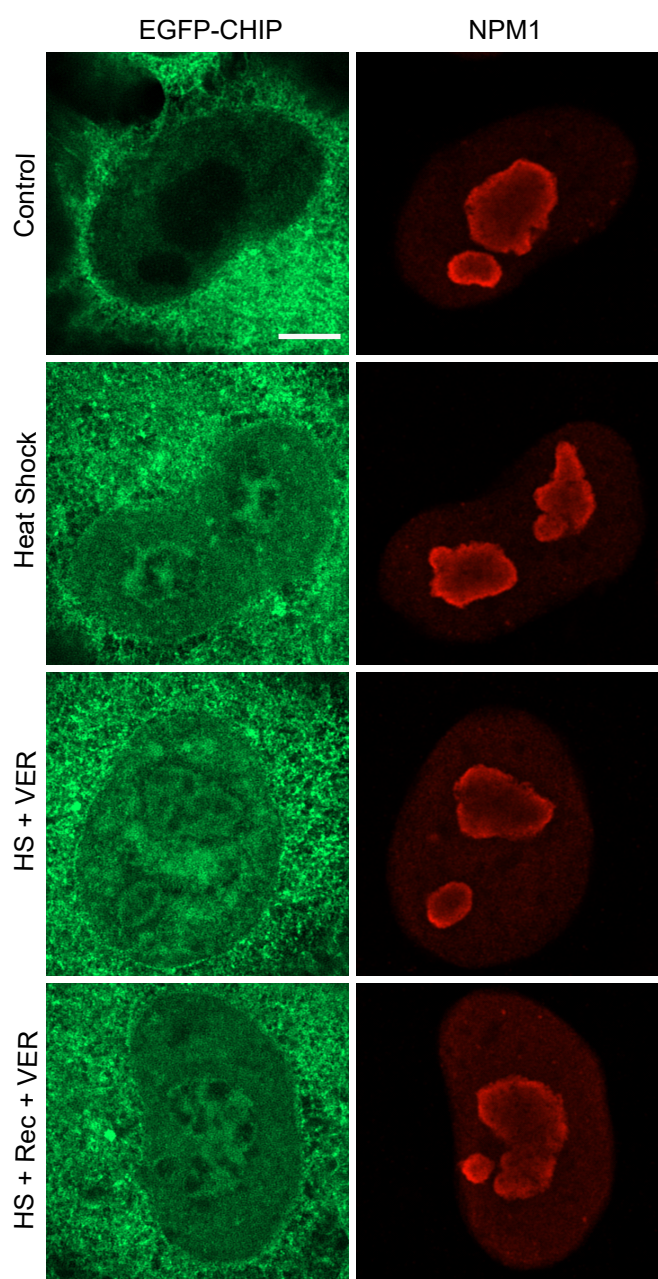


D

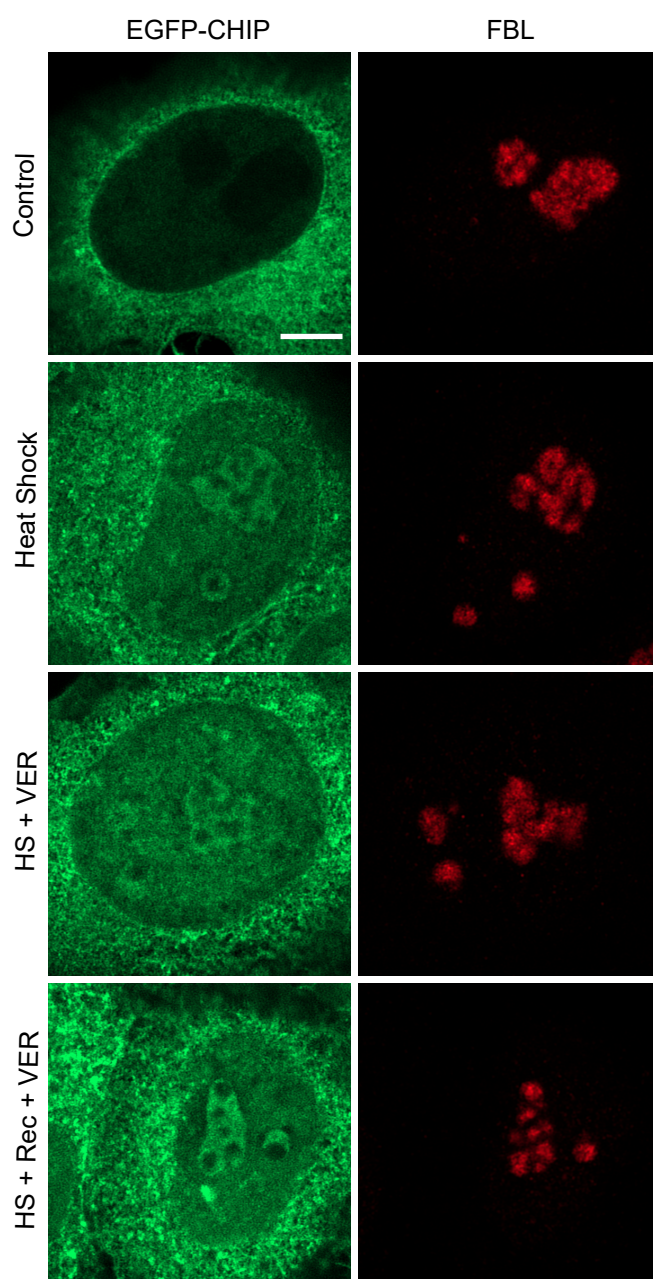




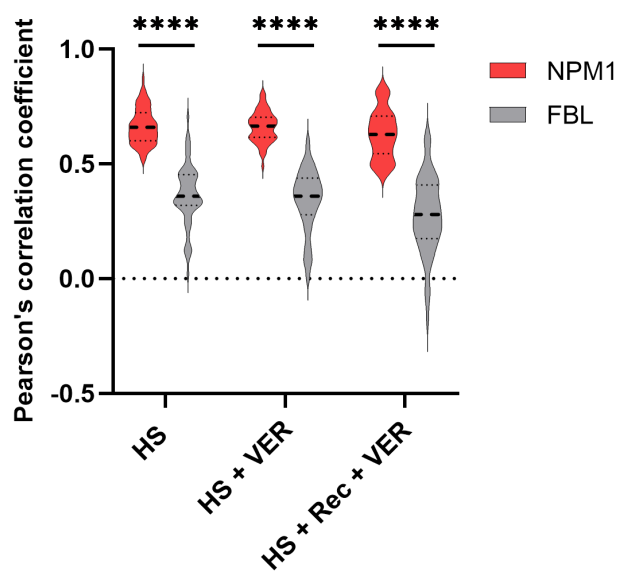
A

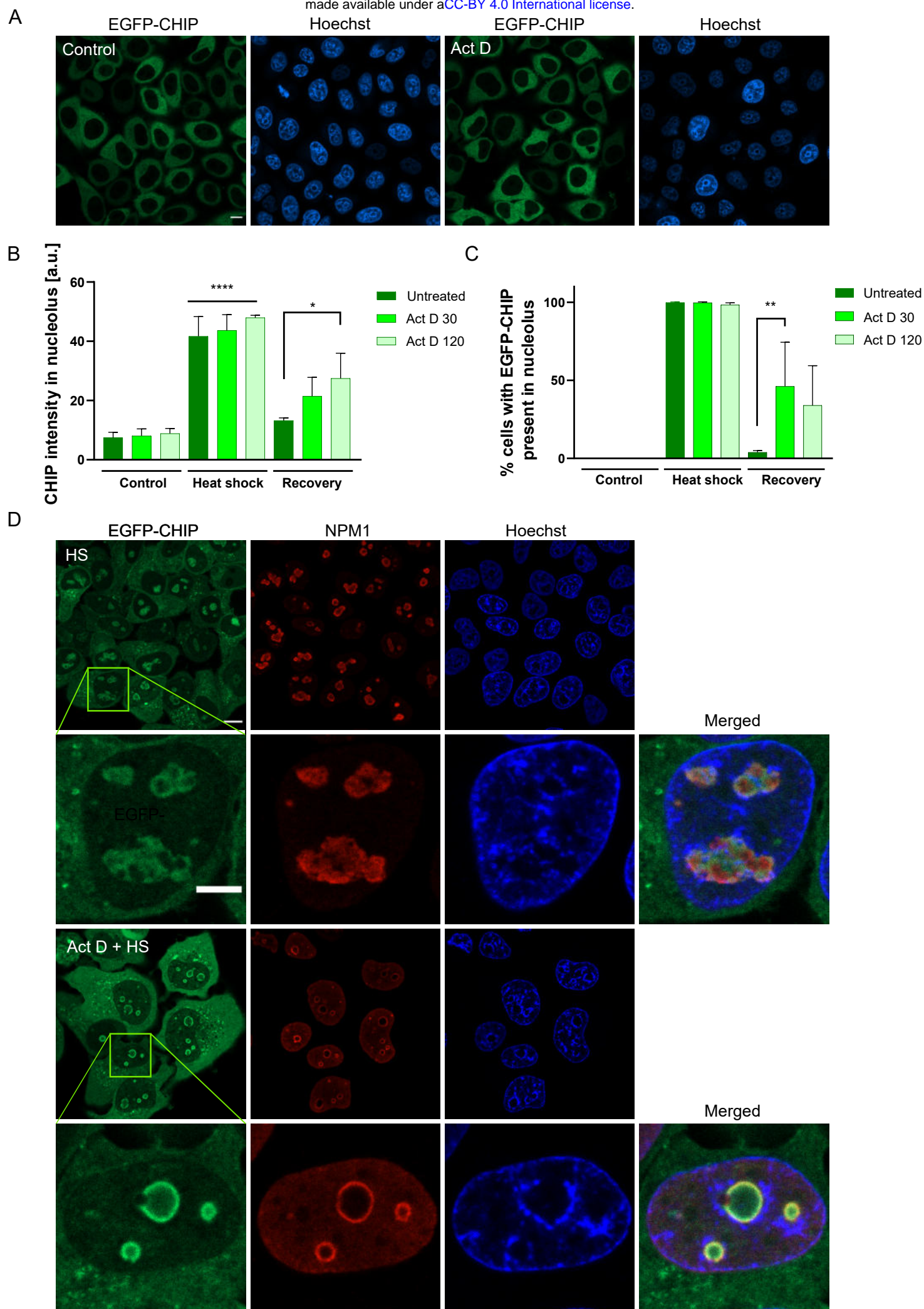


B

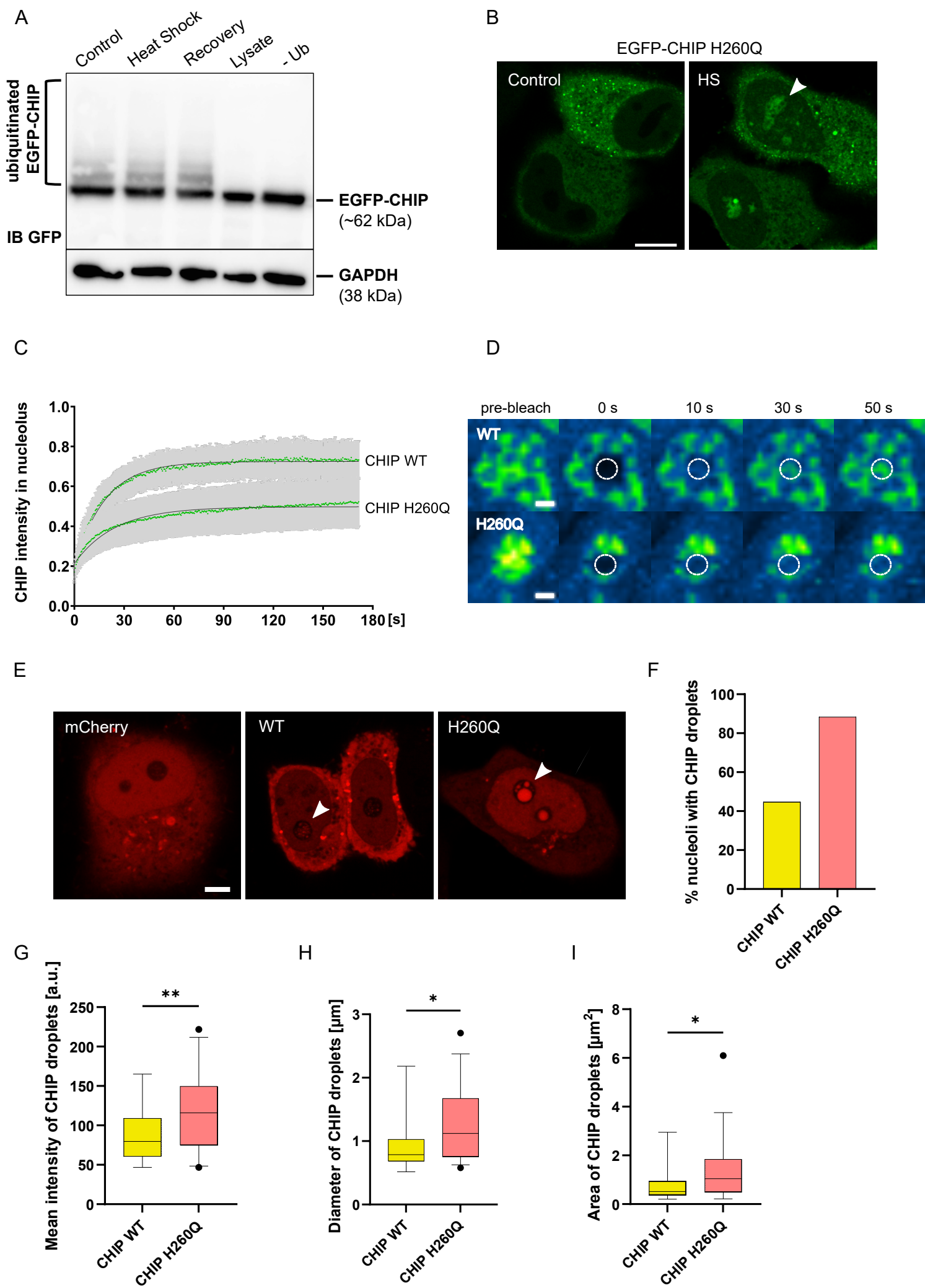


C

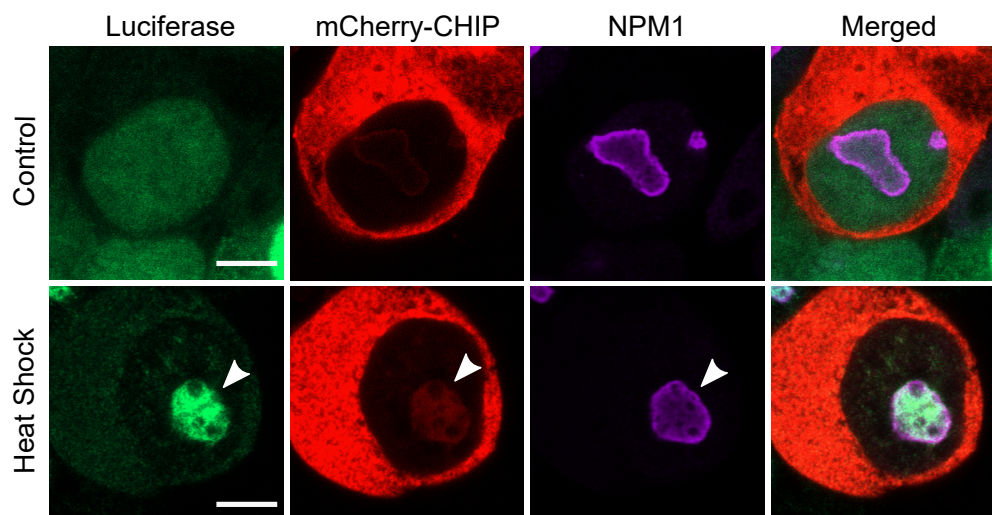




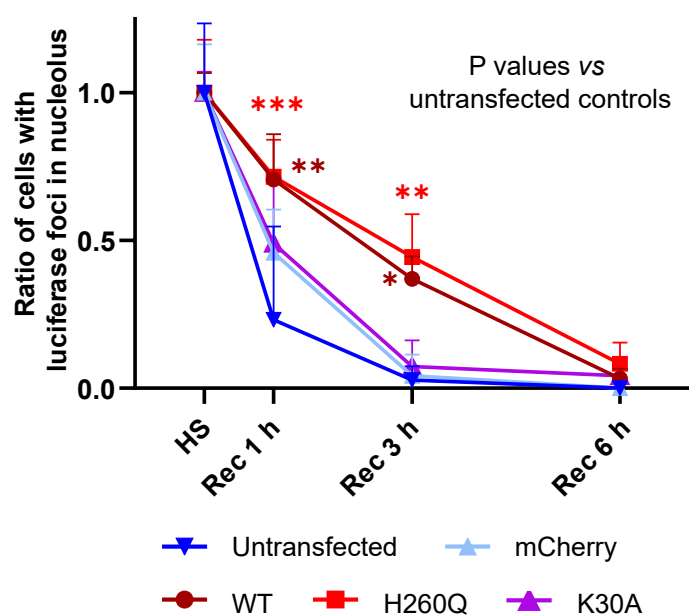
EGFP-CHIP auto-ubiquitination



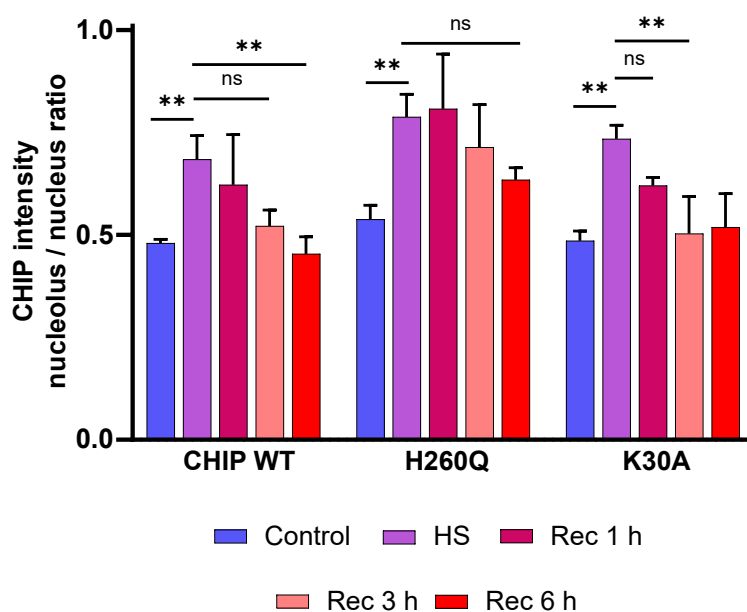
A



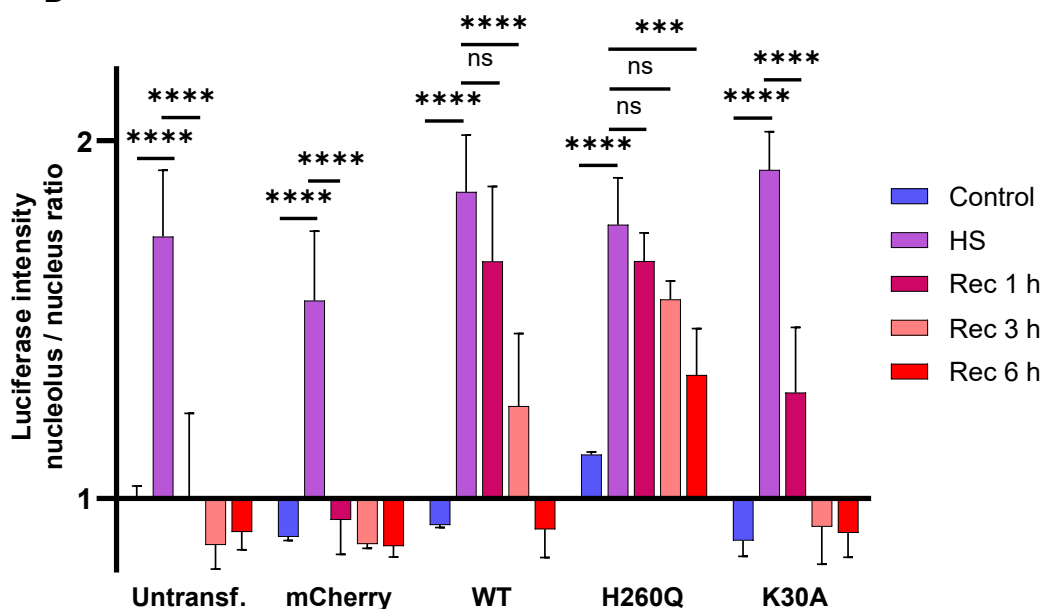
B



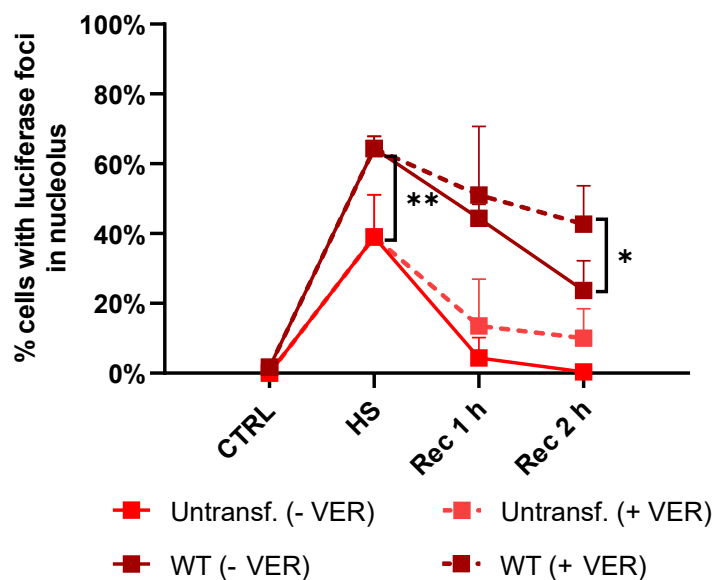
C



D



A



B

